EPA/600/R-93/202
February 1994

A REVIEW AND ASSESSMENT OF FACTORS AFFECTING HYDRAULIC CONDUCTIVITY VALUES DETERMINED FROM SLUG TESTS

by

Gordon K. Binkhorst and Gary A. Robbins
Department of Geology and Geophysics
University of Connecticut
Storrs, CT 06269

Cooperative Agreement
CR-817587-01-1 and CR-817587-02-0

Project Officer

Katrina Varner
Advanced Monitoring Systems Division
Environmental Monitoring Systems Laboratory
Office of Research and Development
Las Vegas, Nevada 89193

ENVIRONMENTAL MONITORING SYSTEMS LABORATORY-LAS VEGAS
OFFICE OF RESEARCH AND DEVELOPMENT
U.S. ENVIRONMENTAL PROTECTION AGENCY
LAS VEGAS, NEVADA 89193-3478

9311-0102amd93

NOTICE

The information in this document has been funded by the United States Environmental Protection Agency under cooperative agreement CR-817587 to the University of Connecticut. It has been subjected to the Agency's peer and administrative review, and it has been approved for publication as an EPA document. Mention of trade names or commercial products does not constitute endorsement or recommendation for use.

PREFACE

This review is part of a cooperative agreement project between the U.S. Environmental Protection Agency, Environmental Monitoring Systems Laboratory, Las Vegas and the University of Connecticut. The overall goal of the project is to improve site assessments for gasoline contamination at service station facilities. This review provides an evaluation of current practices for determining hydraulic conductivity using slug tests in typical monitoring wells. To further evaluate and improve current practices, field and laboratory testing have also been conducted as part of this research. Results of these tests may at this time be found in Binkhorst, G.K. 1992. Evaluation of Slug Test Methods to Determine Hydraulic Conductivity in Unconfined Aquifers, Unpublished M.S. Thesis, Department of Geology and Geophysics, University of Connecticut.

ABSTRACT

The purpose of this study was to evaluate factors that influence hydraulic conductivity values determined by slug tests in typical monitoring wells. Procedures for conducting tests and methods for analyzing test results are summarized and compared. Sensitivity analyses were conducted to identify and evaluate the factors influencing the calculated hydraulic conductivity values for available slug test solutions. These factors include mathematical approximation of the shape of the screen intake, the presence of a less or more permeable well skin, determination of the radius of influence, formation anisotropies and heterogeneities, partial penetration and boundary conditions, and filter sand pack drainage from wells with screens that span the water table (partially submerged well screens). Of these factors, the most significant are the presence of a less permeable well skin, and filter sand pack drainage. The presence of a less permeable well skin around the well screen can result in orders of magnitude under-estimation of the formation conductivity. The effect of a less permeable well skin may be reduced by designing wells to minimize entrapment of fines in the filter pack, and by vigorously developing wells to remove fines associated with well installation. Conducting slug tests in wells with partially submerged screens causes rapid filter sand drainage and extreme reduction of the initial head drop. The initial head reduction can reduce the radius of influence of the test, thereby accentuating well skin effects. Drainage of the filter sand necessitates accounting for the filter sand recharge in the analysis of slug tests. This can be accomplished by using early time slug test data to estimate the specific yield of the filter sand. A method is presented to calculate the filter sand's specific yield from hydraulic head versus time curves for incorporation into existing slug test solutions. However, more reliable hydraulic conductivity values may be obtained from wells with screen sections that remain below the water table during the slug test. This avoids the complexities incurred by filter sand drainage.

CONTENTS

FIGURES

FIGURES (Continued)

LIST OF SYMBOLS AND ABBREVIATIONS

A	Cross-sectional area
A_s	Area of a spherical intake
A_w	Area of a well casing
b	Aquifer thickness
B_l	Length of bailer
B_{or}	Outside radius of bailer
D	Diameter
D'	Distance from lower confining unit to bottom of screen (after Bouwer and Rice, 1976)
D_s	Screen Diameter
H	Hydraulic head
H_l	Length of desaturated filter sand column
$H(t)$	Head drop at any time, t
H_h	Head at the borehole
H_i	Head at the radius of influence
H_o	Initial head drop
H_{oc}	Calculated initial head drop
H_s	Head at the well screen
dH/dl	Hydraulic gradient
H/H_o	Normalized head
k	Formation permeability
K	Hydraulic conductivity
K_{eff}	Effective hydraulic conductivity
K_f	Formation hydraulic conductivity
K_h	Horizontal hydraulic conductivity
K_s	Well skin hydraulic conductivity
k_s	Well skin permeability
K_v	Vertical hydraulic conductivity
$K_{x,y,z}$	Hydraulic conductivity in given Cartesian coordinate
L	Length
L_s	Screen length
L_w	Distance from water table to bottom of screen (after Bouwer and Rice, 1976)
m	Slope
m_a	Anisotropy factor (after Hvorslev, 1951)
n	Porosity
P	Dimensionless discharge (after Widdowson et al., 1990)
Q	Discharge
Q'	Dimensionless discharge (after Dagan, 1978)
Q_f	Flow through formation
Q_h	Flow borehole formation
Q_s	Flow through well screen
r	Radial distance
R_c	Well casing radius
R_{ce}	Effective well casing radius
R_{ci}	Inside radius of well casing
R_{co}	Outside radius of well casing
R_h	Borehole radius
R_i	Radius of influence
R_s	Well screen radius
S	Aquifer storativity
S_f	Shape factor
S_s	Specific storage
S_y	Specific yield
t	Time
T	Transmissivity
T_L	Basic Time Lag
V	Volume
V_b	Volume of bailer
V_c	Volume in well casing
V_s	Volume of drained sand pack
V_w	Volume of water released from sand pack

SECTION 1

INTRODUCTION

The hydraulic conductivity is a measure of a formation's ability to transmit water. The hydraulic conductivity is one of the most important hydrogeologic parameters to be determined at a contamination site. Typical values can vary from 10^2 cm/sec for gravel to 10^{-10} cm/sec for silts and glacial tills (Freeze and Cherry, 1979). Estimates of groundwater flow velocities, well yields, and rates of contaminant migration will be directly proportional to the value of the hydraulic conductivity and associated errors in determining this value. Accurate determination of hydraulic conductivity and its spatial distribution are essential for modeling both adjective and dispersive contaminant migration. An order of magnitude error in the conductivity would result in an equal magnitude of error in predicting the position of an adjective front of a contaminant plume. A distribution of varying conductivities at a site may create preferential pathways and result in large scale dispersion of contaminated groundwater (Molz et al., 1988). Other important uses of hydraulic conductivity are: design of remediation wells, evaluating capture zones of remediation or production wells, and assessing risk associated with subsurface contamination.

The hydraulic conductivity can be determined by several laboratory and field methods. Laboratory methods involve collecting either an undisturbed core sample, or remolding a sample to its approximate in situ bulk density. These samples can be tested by either constant or falling head permeameter tests. Core samples, collected in a vertical orientation, are difficult to collect and preserve in a truly undisturbed manner. Hydraulic conductivity values obtained in vertically oriented cores can be strongly affected by anisotropies associated with stratification. Therefore, laboratory tests may not be reflective of field conditions, where flow may be predominantly horizontal. Remolding of samples may provide a better overall estimate, but disturbs the natural properties of the sediment, such as layering, small scale structures and packing (Taylor et al., 1990). Rough estimates of hydraulic conductivities may also be obtained from core samples based on correlations with grain size distribution (Sheperd, 1989).

Field methods for determining the hydraulic conductivity include tracer, pump and slug tests. Tracer tests can provide both hydraulic conductivity and dispersion characteristics at the scale of the injection and monitoring points. However, tracer tests involve injecting a foreign, readily detectable compound, such as sodium bromide or a radionuclide into the aquifer. Both conducting and analyzing these tests can be complex, time-consuming and expensive. Pumping tests generally provide information on the large scale hydrogeologic characteristics, hydraulic conductivity and storage properties of an aquifer (Butler, 1990). Pumping tests can be expensive, of long duration, require one or more observation wells for data analysis, and involve disposal of large quantities of contaminated water. Slug tests may provide spatially discrete values of the hydraulic conductivity using a single well point or multi-level sampler (Widdowson et al., 1990). They are relatively quick, inexpensive, and involve removal of little or no potentially contaminated water. As such, slug tests in

groundwater monitoring wells are the most widely used method by the environmental consulting industry for determining the hydraulic conductivity at contamination sites.

A slug test is performed by creating an instantaneous hydraulic head difference between the well and the adjacent formation. This head difference can be created by the 'instantaneous' addition or removal of either a slug of water or a solid slug (mandrel displacement). The recovery of this head difference is subsequently monitored by recording the change in water level in the well with time using either a water level indicator or pressure transducer. The head difference generally recovers exponentially or log-linearly with time (Dax, 1987). The slope of the logarithm of head versus time relationship can be used to determine the hydraulic conductivity. Interpretation of slug test data to derive a hydraulic conductivity value is a function of the geometry of the well, hydrogeologic parameters, and well and borehole conditions. Geometric parameters of the well include casing, screen, and filter pack dimensions. These parameters are incorporated as "shape factors" into mathematical solutions in order to analyze slug tests. Hydrogeologic parameters which may affect slug tests include: confined versus unconfined conditions; degree of screen section penetration into the aquifer; aquifer storativity; presence and proximity of semi- or impermeable boundaries; anisotropy of aquifer properties; and the radius of influence of the test. Well and borehole conditions include skin effects due to borehole disturbance, the presence of a filter pack around the screen, well storage, and well friction losses. Conducting and interpreting slug tests in typical groundwater monitoring wells with screens and filter packs spanning the water table in unconfined aquifers can be additionally complicated by the drainage and subsequent resaturation of the filter pack.

A typical monitoring well in which slug tests are commonly conducted by the environmental consulting industry is shown in Figure 1. A typical well consists of a 5.08 cm (2 inch) screen installed in a 22.86 cm (9 inch) diameter hole in an unconfined aquifer. The annular space between the well screen and the borehole is typically filled with a filter or sand pack of fine- to coarse-grained sand. The well screen is commonly partially submerged, i.e., both the screen and the filter pack extend from above the water table to some depth below the water table. In order to analyze a slug test conducted in this type of well, the water table is generally considered to be a no flow boundary, i.e., no drawdown occurs in the water table adjacent to the well. A partially submerged well screen creates several additional problems in both conducting and analyzing slug tests. These problems include filter pack drainage, a variable intake length during water level recovery, re-saturation of an unknown portion of the filter pack, a small head difference after filter pack drainage, and potential propagation of a cone of depression.

Analysis of slug test data is based on application of either Darcy's Law and the Thiem Equation for the case of no storage as summarized by Hvorslev (1951) or numerical solutions to the partial differential equation for non-steady radial flow with aquifer storage as first proposed by Ferris and Knowles (1954) and later by Cooper et al. (1967). Both approaches have been adapted to incorporate such effects as borehole skin, partial penetration, anisotropy, impermeable boundaries, the radius of influence, and the intake geometry (e.g., Bouwer and

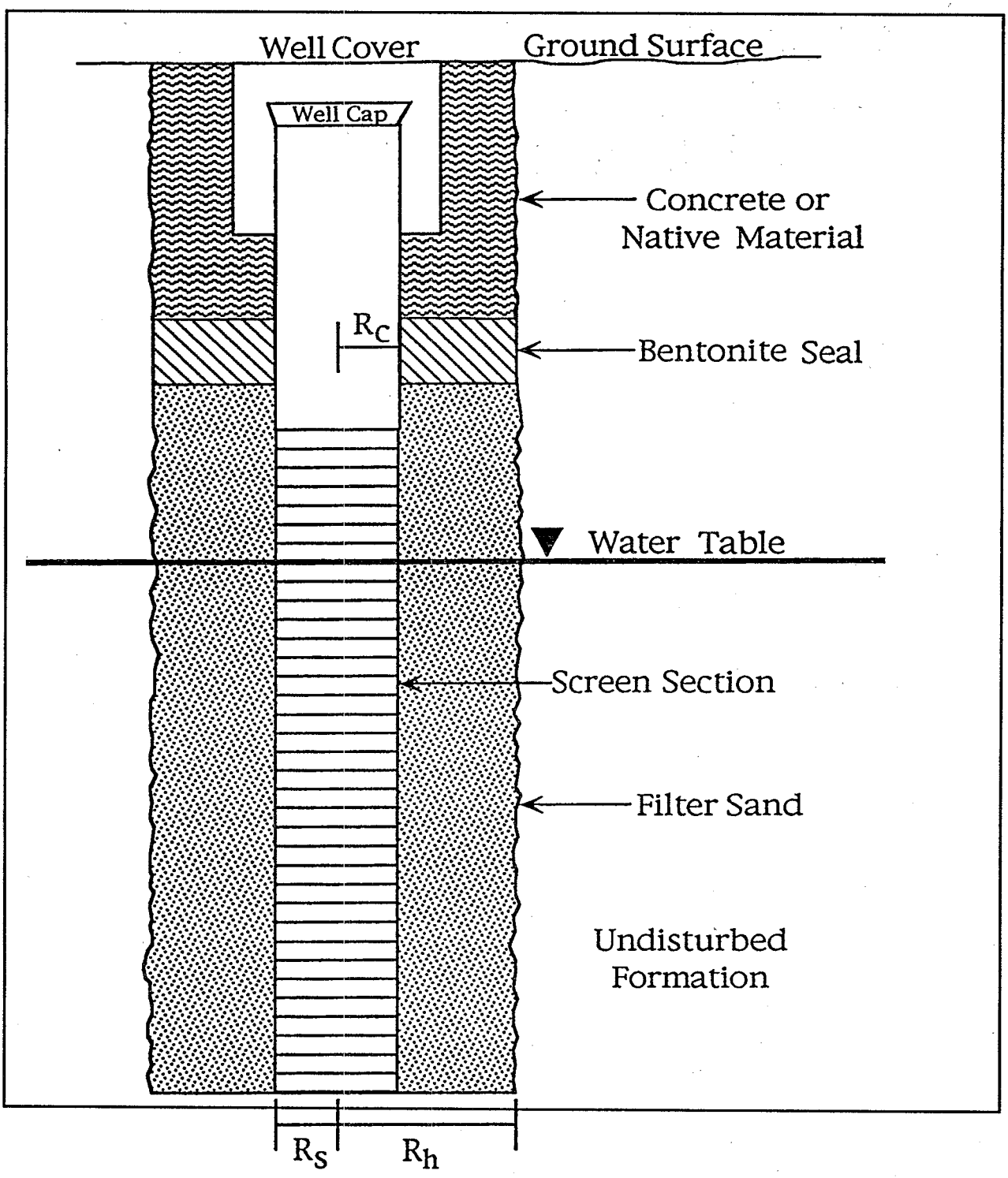

Figure 1. Typical ground water monitoring well with partially submerged well screen. R_s = screen radius; R_h = borehole radius; R_c = well casing radius.

Rice, 1976; Braester and Thunvik, 1984; Widdowson et al., 1990). A review of the derivation and application of the most widely used models for determining hydraulic conductivity from slug tests in both confined and unconfined aquifers is contained in Chapter 2. Chapter 3 is an assessment of the factors affecting slug tests and provides methods for accounting for these factors. Chapter 4 provides recommendations for conducting and interpreting slug tests.

SECTION 2

ANALYSIS OF SLUG TEST DATA

Slug test analysis techniques can be differentiated into two main categories based on whether the aquifer is unconfined or confined. For the unconfined case, the solution is based on steady state flow to the well due to a hydraulic gradient, and is derived using Darcy's Law or the Thiem Equation integrated over time. In the case of a confined aquifer, the solutions incorporate the release of water from storage due to compression/expansion of the aquifer matrix and expansion/compression of the water. The confined solutions are based primarily on numerical solutions of the transient saturated flow equation. If the storage coefficient is low, or the amount of water released from storage is small or instantaneous, then the solutions for the confined case will converge on the solutions for the unconfined case. The available solutions for both the unconfined and confined cases are presented below.

SLUG TEST INTERPRETATION IN UNCONFINED AQUIFERS

Derivation of the hydraulic conductivity from a slug test in a well in an unconfined aquifer using a modified form of Darcy's Law was first proposed by Kirkham (1946), following the auger hole seepage theory of Hooghoudt (1936). Darcy's Law (1) states that one dimensional flow through a porous media of cross-sectional area (A) due to a hydraulic gradient (dH/dl) is proportional to the hydraulic conductivity (K).

$$Q = -K\, dH/dl\, A \tag{1}$$

To illustrate the derivation of a slug test solution using Equation 1, consider steady state flow to a spherical intake in an unconfined, homogeneous and isotropic aquifer of infinite extent. Darcy's Law in spherical coordinates for this case may be expressed as:

$$Q = -K \frac{dH}{dr} A_s \tag{2}$$

In this form, the cross-sectional area has been replaced by the area of a spherical intake, A_s, equal to $4\pi r^2$. Rearranging and integrating Equation 2 yields:

$$\int_{R_s}^{\infty} (dr/r^2) = -4\pi K \int_{H}^{0} dH \tag{3}$$

The solution of Equation 3 for steady state flow is:

$$Q = -K4\pi R_s H \tag{4}$$

In Equation 4, R_s is the radius of a spherical intake (for naturally developed wells with no filter pack, R_s is the screen radius; for wells with a filter sand pack, R_s should be the borehole radius, R_h). Imagine that this spherical intake is connected to a vertical standpipe of radius R_c (where $R_c << R_s$). Consider a slug test being performed in the standpipe. During water level recovery, the flow rate, Q, into the spherical intake is equal to the rise (or fall) of the water level with time in the standpipe (i.e., $\pi R_c^2 dH/dt$). Substituting for Q, rearranging, and integrating (5) over time and head yields (6). Equation 6 is the equation for determining the hydraulic conductivity from slug test data collected from a well with a spherical intake.

$$\int_{H_1}^{H_2} dH = -\frac{K 4\pi R_s}{\pi R_c^2} \int_{t_1}^{t_2} dt \qquad (5)$$

$$K = -\frac{\pi R_c^2}{4\pi R_s} \frac{\ln(H_2/H_1)}{(t_2-t_1)} \qquad (6)$$

Equation 6 is exact for a spherical intake assuming the aforementioned conditions, no cone of depression around the well, and a fully submerged screen section at all times. The term $4\pi R_s$ in Equation 6 is called the shape factor (S_f) for a spherical intake. As such, (6) can be re-written as:

$$K = -\frac{\pi R_c^2}{S_f} \frac{\ln(H_2/H^1)}{(t_2-t_1)} \qquad (7)$$

Equation 7 is the general form of slug test solutions. For the idealized case of a spherical intake, S_f is a simple term. For other intake geometries, S_f can be quite complex, and no simple mathematical solution can be derived. Therefore, shape factors for Equation 7 have been approximated by closed form analytical methods, 2-D and 3-D electrical analog methods, and numerical methods for a wide variety of well and aquifer geometries. A full presentation of currently available shape factors and their implications will be presented in Chapter 3.1.

The two most common shape factors for use in (7) which are applicable to slug tests in unconfined aquifers are 1) the '1/2 ellipse' shape factor for flow to a cylindrical intake open below an impermeable boundary and 2) the full ellipse shape factor for flow to a cylindrical intake in an infinite aquifer. The applicable well and aquifer geometries are depicted in Figure 2. The earliest derived shape factor for the 1/2 ellipse model of a cylindrical intake, with length L_s and radius R_s, open below an impermeable boundary was first approximated by Forchiemer (1930) and Dachler (1936) using closed form analytical solutions of the Laplace

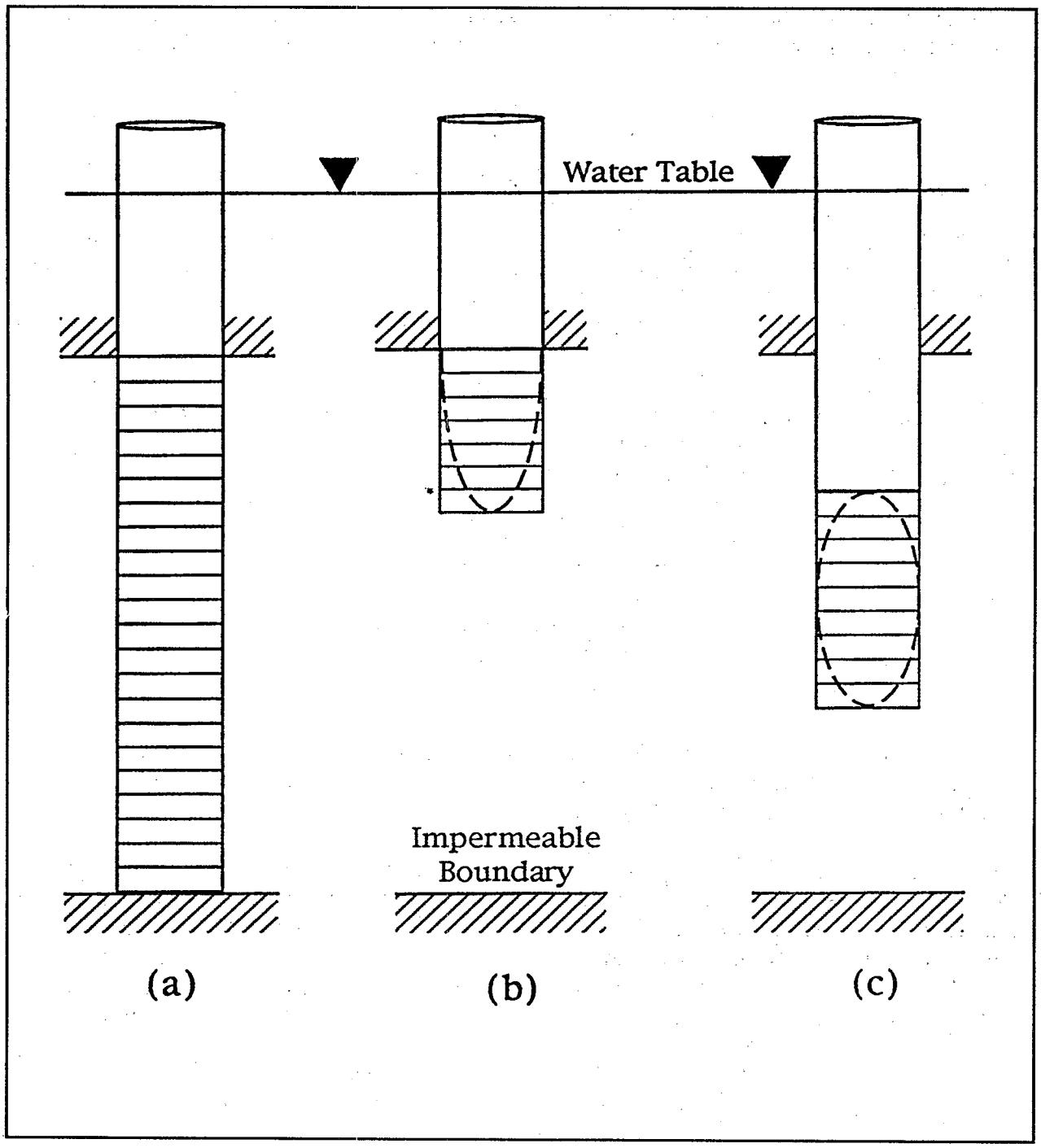

Figure 2. Slug test geometries for (a) doughnut, (b) 1/2 ellipse, and (c) full ellipse models.

Equation for an ellipsoid equivalent of a cylindrical injection zone. The solution is based on flow from a line source for which the equipotential surfaces are semi-ellipsoids:

$$S_f = \frac{2\pi L_S}{\ln(L_s/R_s + \sqrt{1 + (L_s/R_s)^2})} \quad (8)$$

The denominator of Equation 8 can be simplified to $\ln(2L_s/R_s)$ for $L_s/R_s > 4$, resulting in error of less than 1% (Hvorslev, 1951). It is emphasized by Dachler (1936) that this formula for the 1/2 ellipse shape factor can provide only approximate results when applied to a cylindrical intake open below an impermeable boundary. The full ellipse shape factor applies to a cylindrical intake in an infinite medium (i.e., no boundaries). For this case, the assumption was made that flow lines are symmetrical with respect to a horizontal plane through the center of the intake, and then the formula from (8) was applied to the upper and lower halves of the intake to obtain the following shape factor:

$$S_f = \frac{2\pi L_S}{\ln(L_s/2R_s) + \sqrt{1 + (L_s/R_s)^2}} \quad (9)$$

Similar to Equation 8, the denominator of Equation 9 can be simplified to $\ln(L_s/R_s)$ for $L_s/2R_s > 4$. If the ratio of screen length to screen radius is unity in (9), the shape factor is approximately the same as that for a spherical intake.

While the 1/2 ellipse and full ellipse models account for both horizontal and vertical flow to the well screen, as the screen length gets increasingly larger relative to the well diameter, the influence of vertical flow diminishes relative to horizontal flow. As stated in Hvorslev (1951), the accuracy of these shape factors probably decrease with increasing values of L_s/R_s. Assuming that for most monitoring well geometries, $L_s/2R_s > 4$, and substituting (8) and (9) into (7), yields the 1/2 ellipse model (10) and the full ellipse model (11), respectively:

$$K = -\frac{(R_c^2)\ln(2L_s/R_s)}{2L_s}\,\frac{\ln(H_2/H_1)}{t_2-t_1} \quad (10)$$

$$K = -\frac{(R_c^2)\ln(2L_s/R_s)}{2L_s}\,\frac{\ln(H_2/H_1)}{t_2-t_1} \quad (11)$$

If flow is restricted to radial flow, this may be described by the Thiem Equation. The model geometry for this case, the doughnut model, is also presented in Figure 2. The radial flow assumption is ideal for an aquifer bounded at the top and bottom by an impermeable boundary, but may similarly apply to a partially penetrating well in an anisotropic aquifer were the horizontal conductivity is significantly greater than the vertical. The doughnut model is frequently applied to wells containing a partially submerged screen section. This implicitly assumes radial flow and no drawdown of the water table adjacent to the well.

Derivation of the doughnut model parallels the derivation of the models described above. For this case, the area of a sphere in Equation 2 is replaced by the area of a cylinder, $2\pi R_s L_s$. The resulting equation is then integrated from R_s to R_i, the radius of influence. The remaining derivation follows the steps above. The resulting doughnut model is:

$$K = - \frac{(R_c^2) \ln(R_1/R_s)}{2L_s} \quad \frac{\ln(H_2/H_1)}{t_2 - t_1} \qquad (12)$$

The use of this model requires the determination or estimation of a radius of influence. The shape factor for this model is:

$$Sf = \frac{2\pi L_s}{\ln(R_i/R_s)} \qquad (13)$$

The radius of influence (R_i) appears equivalent to screen length (L_s) of the full ellipse model, or twice the screen length of the 1/2 ellipse model, as was pointed out by Bouwer and Rice (1976). The shape factors for the elliptical solutions are approximations, whereas the doughnut shape factor is exact for the model geometry. In the derivation of this model, it was necessary to reduce the constant head radius from infinity to R_i in order to keep head finite. Theoretically, the radius of influence is infinite in an aquifer of infinite extent. Practically, a slug test involves small quantities of water and lasts for a short period of time. Consequently, the radius of influence must be relatively close to the well. The radius of influence of a slug test has been defined and evaluated by a number of authors, e.g., Hvorslev, 1951; Bouwer and Rice, 1976; Dagan, 1978; Sageev, 1986; Dax, 1987; Karasaki et al., 1988; Chirlin, 1989. A full discussion of the radius of influence and its implications is included in Chapter 3.2.

Application of the above models to determine the hydraulic conductivity from slug test data may be conducted in three ways, by linear regression, using two representative head and corresponding time measurements, and by the Hvorslev (1951) Basic Time Lag method. The recovering head in the well following either a slug out (or in) test is equivalent to the changing (recharging or discharging) water level in the well. The equilibrium water level is taken as a fixed datum point. A depiction of the recovering head following a slug out test is included as Figure 3. The head versus time data may then be plotted on semi-log paper, or

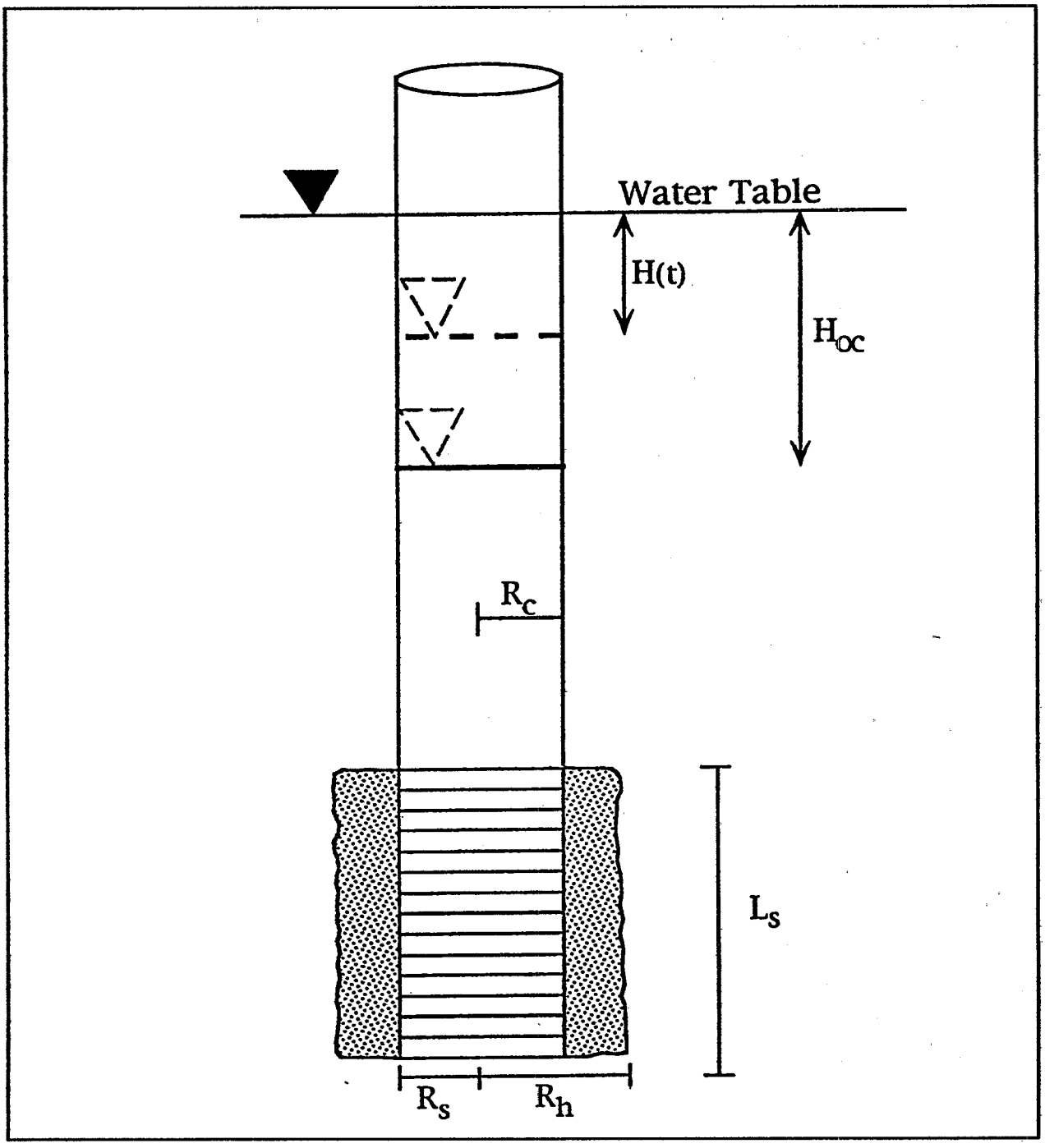

Figure 3. Hydraulic head representation following a slug out test. L_s = screen length, R_h = borehole radius, R_s = well screen radius, R_c = well casing radius, H_{oc} = calculated initial drawdown, and H(t) = head at any time t.

similarly, the natural log (In) of head versus time may be plotted on normal paper. Figure 4 is an example of such a plot for a well with a fully submerged well screen. The plot exhibits log-linear recovery in early time, then tails off. The tailing off of the recovery curve in late time is most likely due to the recovery of a cone of depression in the adjacent formation, i.e., an ever diminishing hydraulic gradient between the well and the formation. It may also be accentuated in wells with partially submerged screens by the resaturation of the filter sand pack. The slope of the log-linear portion of the recovery curve is directly proportional to the product of the shape factor and the hydraulic conductivity, and inversely proportional to the square of the radius of the casing in which the water level is recovering. This may be seen by rearranging Equation 7 in log-linear form, ln y = mx + ln b yielding Equation 14:

$$\ln H_2 = -\frac{KS_f}{\pi R_c^2}(t_2-t_1) + \ln H_1 \qquad (14)$$

The slope of (14) is equivalent to:

$$\text{slope} = m = -\frac{KS_f}{\pi R_c^2} = \frac{\ln(H_2/H_1)}{t_2-t_1} \qquad (15)$$

and the radius of the casing in which the water level is rising, the hydraulic conductivity may be calculated. Similarly, the hydraulic conductivity can be calculated using (14) and two pairs of head and time measurements. Alternatively, the 'Basic Time Lag' method can be used as developed by Hvorslev (1951). This method is a simple graphical manipulation of (7), and can facilitate incorporation of differing shape factors. By rearranging (7) and substituting the term A_w for the area of the casing:

$$t_2-t_1 = -\frac{A_w}{KS_f}\ln(H_2/H_1) \qquad (16)$$

Setting $t_1 = 0$, $t_2 = t$, $H_2 = H$, and $H_1 = H_o$ (the initial head drop):

$$t = -\frac{A_w}{KS_f}\ln(H/H_o) \qquad (17)$$

A plot of H/H_o (normalized head) versus time on semi-log paper, as shown in Figure 5, is generated for this method. The initial head drop (H_o) should be established as the Y axis intercept of the linear portion of the semi-log plot of head versus time data (Figure 4). Calculation of the initial head drop using the volume of the removed slug or basing the initial

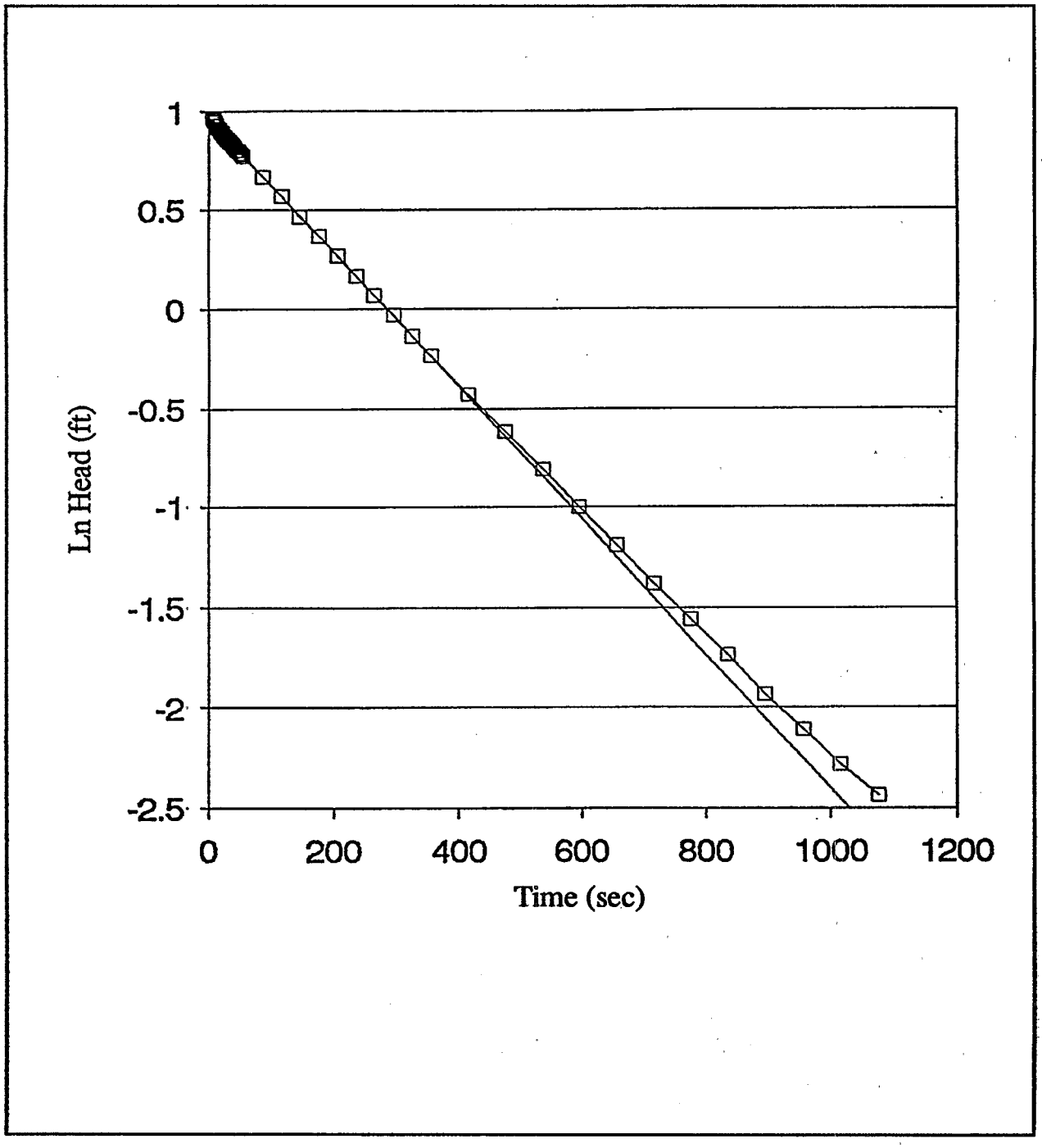

Figure 4. Typical slug out test recovery curve for a monitoring well with a fully submerged well screen. Well TJ-1; UCONN Beach Hall; March 27, 1991. After Binkhorst, 1992.

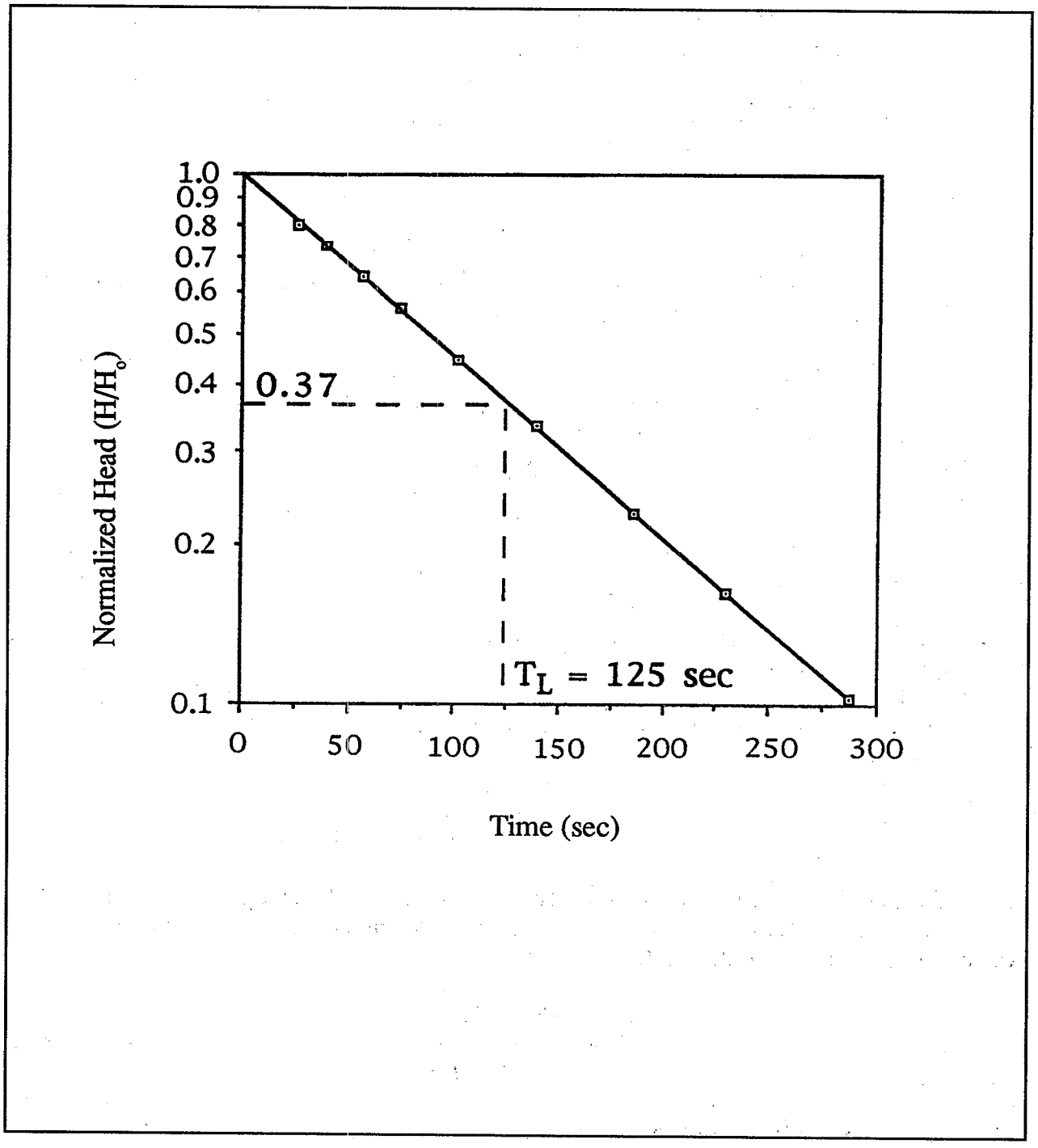

Figure 5. Hvorslev Basic Time Lag method. H = head at given time, H_o = initial head drop, and T_L = the Basic Time Lag.

head drop on the first collected readings may incorporate errors stemming from filter pack drainage, water level disturbance, and lack of accuracy in early time measurements. At $H/H_o = 0.37$, at which time 63% of the initial head drop has dissipated, $\ln(H/H_o) = -1$. The time (t) at which this occurs is termed the Basic Time Lag (T_L) and (17) becomes:

$$K = \frac{A_w}{S_f T_L} \tag{18}$$

From Figure 5, T_L may be graphically determined. Aside from facilitating the use of different shape factors, no other advantage is gained from this method.

In addition to the methods summarized by Hvorslev (1951), Dagan (1978) presented an analytical solution for steady state flow to partially penetrating wells in unconfined aquifers. Dagan's solution considers the effects of vertical and horizontal flow, but assumes no storage and a constant head condition at the water table. The solution is only applicable for cases where the screen intake length is greater than 50 times the well radius. Following Muskat (1937), Dagan obtained the steady state flow solution by assuming flow is generated by a continuous distribution of sources of unknown strength along the well axis. He used the theory of images to account for a lower impermeable boundary. The intake length is divided into a finite number of intervals and the total flow to the well is calculated as the sum of the flow to each interval. Solving a series of equations, Dagan generated values of dimensionless discharge (Q') versus $\log(L_s/R_s)$ for different degrees of partial penetration of the screen. He compared his method for packers with slug test and Bouwer and Rice (1976) solutions as is shown in Figure 6 (after Dagan, 1978). The dimensionless discharge Q' is:

$$Q' = \frac{Q}{2\pi K L_s H} \tag{19}$$

Using the determined dimensionless discharge based on the well and aquifer geometry, and the slope of the natural log of head versus time curve, the hydraulic conductivity may be calculated using Dagan's method from:

$$K = -\frac{R_c^2}{2Q'L_s}\frac{\ln(H_2/H_1)}{t_2-t_1} \tag{20}$$

SLUG TEST INTERPRETATION IN CONFINED AQUIFERS

A head difference from a slug test in a confined aquifer results in flow to the well not only due to the induced hydraulic gradient, but also from a release of water from storage. The release of water from storage due to a head difference during a slug out test is due to

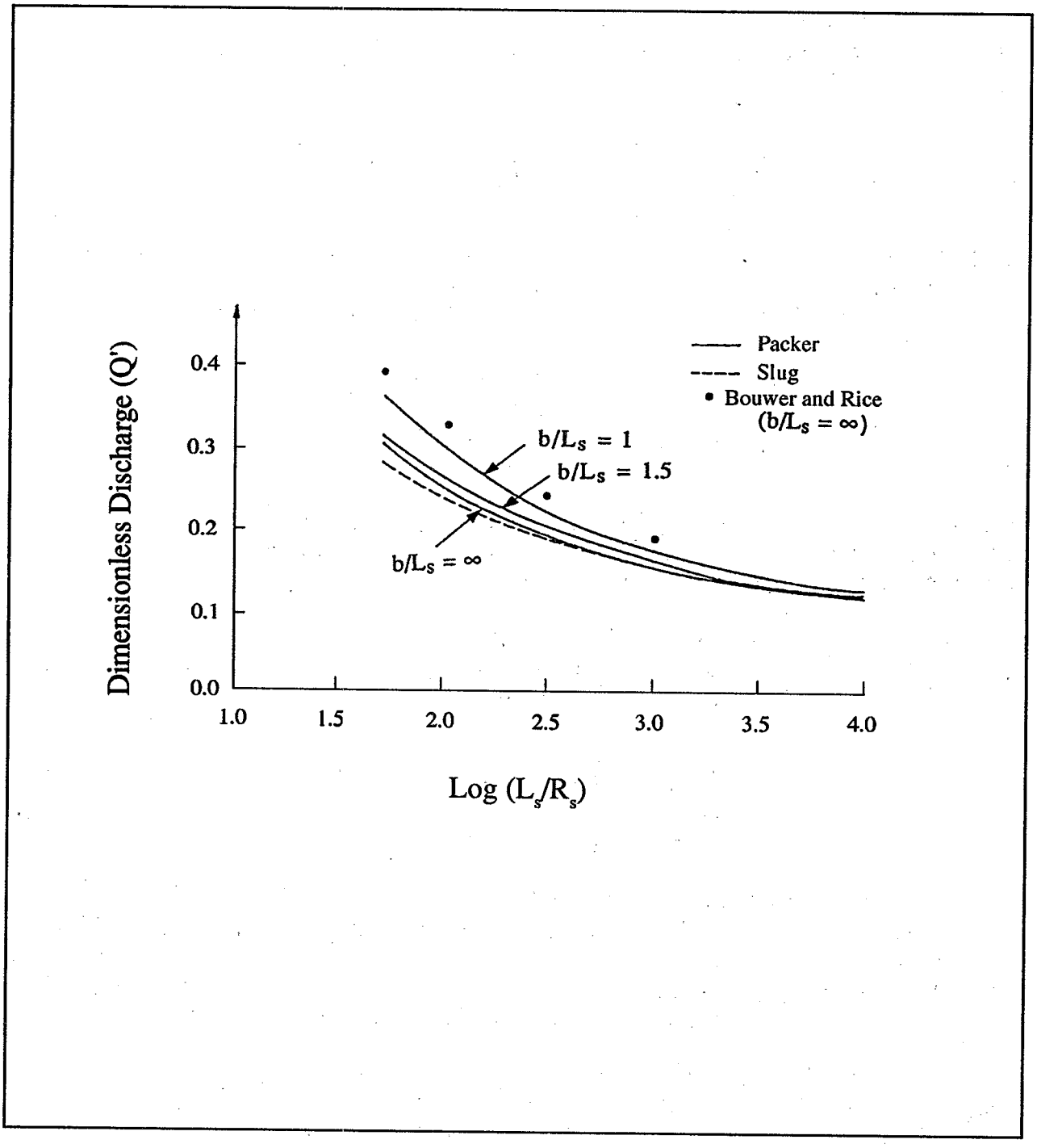

Figure 6. Comparison of dimensionless discharge (Q') curves for different slug test models. b = aquifer thickness, R_s = well screen radius, and L_s = well screen length. After Dagan, 1978.

compression of the aquifer matrix and expansion of the water. Flow to a well in a confined aquifer is governed by:

$$\frac{d}{dx}\left(K_x\frac{dH}{dx}\right)+\frac{d}{dy}\left(K_y\frac{dH}{dy}\right)+\frac{d}{dz}\left(K_z\frac{dH}{dz}\right)=S_s\frac{dH}{dt} \tag{21}$$

where S_s is equal to the specific storage and $K_{x,y,z}$ is equal to the hydraulic conductivity in the x, y, and z directions of the given Cartesian coordinate system. For the case of a homogeneous and isotropic media ($K_x = K_y = K_z = K$), Equation 21 becomes:

$$\frac{d^2H}{dx^2}+\frac{d^2H}{dy^2}+\frac{d^2H}{dz^2}=\frac{S_s}{K}\frac{dH}{dt} \tag{22}$$

For the case of a fully penetrating well in a confined aquifer of thickness b, Equation 22 becomes 23 in Cartesian coordinates or Equation 24 in radial coordinates, where the storativity, $S = S_s b$ and transmissivity, $T = Kb$:

$$\frac{d^2H}{dx^2}+\frac{d^2H}{dy^2}=\frac{S}{T}\frac{dH}{dt} \tag{23}$$

$$\frac{1}{r}\frac{dH}{dr}+\frac{d^2H}{dr^2}=\frac{S}{T}\frac{dH}{dt} \tag{24}$$

As shown in Lohman (1972), the equations for transient, saturated flow in confined aquifers, shown here as Equations 21-24, are based on a combination of Darcy's Law, the clarification of hydraulic potential by Hubbert (1940), the concepts of aquifer elasticity by Meinzer (1923), and effective stress by Terzaghi (1925). The classical development of these equations was first completed by Jacob (1940), and can be found in complete form in Jacob (1950).

Ferris and Knowles (1954) first applied these equations to determine the hydraulic conductivity from slug tests in confined aquifers by approximating the well with an instantaneous line source. However, Bredehoeft et al. (1966) demonstrated by electrical analog that the solution of Ferris and Knowles was only satisfactory when time was large enough for the ratio of head to initial head (H/H_o) to be less than 0.0025. The error associated with Ferris and Knowles method is due to the approximation of the well as a line source.

Cooper et al. (1967) solved Equation 24 numerically with the Laplace transform with respect to time for a finite diameter, fully penetrating well in a confined aquifer. The Cooper et al. method comprises, perhaps, the most commonly used solution for interpretation of slug tests in confined aquifers. Using the inverse transform, as provided by Carslaw and Jaeger (1959) for the analogous heat flow problem, Cooper et al. showed:

$$H = 8H_o \frac{\alpha}{2} \int_0^{\infty} \exp\left(\frac{-Bu^2}{\alpha}\right) \frac{du}{u\nabla u} \qquad (25)$$

where:

$\alpha = R_s^2 S / R_c^2$
$B = Tt / R_c^2$
u = Variable of integration
$\nabla u = (uJ_o(u) - 2\alpha J_1(u))^2 + (uY_o(u) - 2\alpha Y_1(u))^2$
J_n = Bessel function of the first kind, n^{th} order
Y_n = Bessel function of the second kind, n^{th} order

Values of H/H_o versus Tt/R_c^2 for five different values of α were obtained by numerical simulation of Equation 25 and were plotted as a family of semi-logarithmic curves. In order to obtain a transmissivity and storage coefficient, slug test data are plotted as H/H_o versus time on semi-log paper at the same scale as the Cooper et al. type curves. The slug test data curve is then superimposed on the best fit type curve and a value of t is determined at $T_t/R_c^2 = 1.0$. Each type curve is assigned a value of α from 10^{-1} to 10^{-5} in Cooper et al. (1967); the range of α was extended for cases of low storativity from 10^{-5} to 10^{-10} by Papadopulos et al. (1973). A combination of the Cooper et al. curves and the Papadopulos et al. curves is included as Figure 7 (after Papadopulos et al., 1973). The transmissivity and storativity may then be calculated from Equations 26 and 27 respectively:

$$T = \frac{R_c^2}{t} \qquad (26)$$

$$S = \frac{R_c^2}{R_s^2} \alpha \qquad (27)$$

Cooper et al. concluded that the determination of storage coefficients by this method was of questionable reliability due to the similarity of the shapes of the type curves. A shift to an adjacent type curve results in an order of magnitude change in α, and consequently in the value of S. According to the authors, the value of T is much less sensitive to this problem. According to Papadopulos et al. (1973), an analysis in the range of $\alpha < 10^{-5}$ indicates that if the

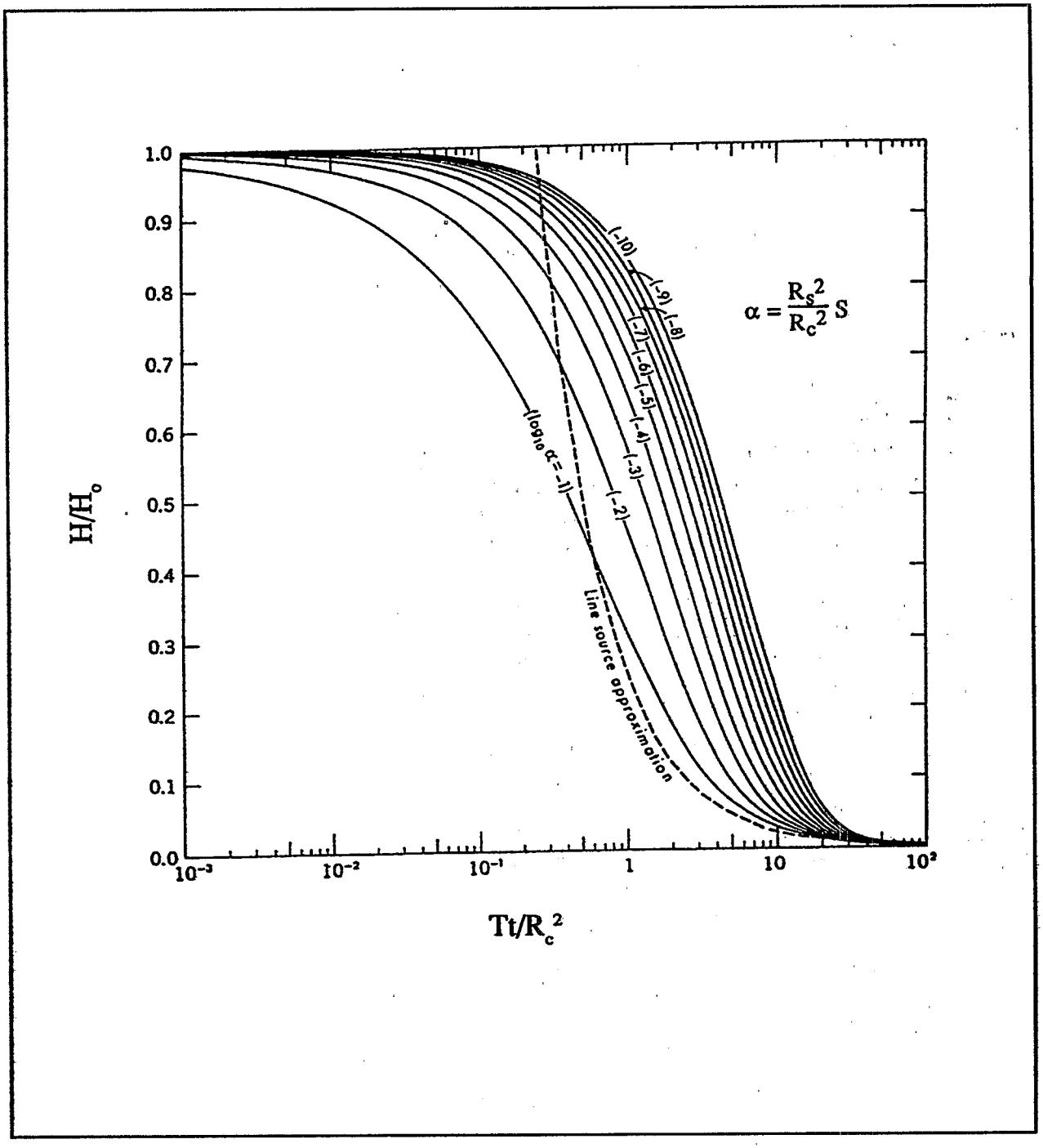

Figure 7. Confined aquifer type curves. After Papadopulos et al., 1973.

value of α for the chosen type curve is within two orders of magnitude of the actual value, the error in the determined value of T would be less than 30%.

Slug tests in multi-level wells with small screened sections in anisotropic confined aquifers was considered by Widdowson et al. (1990) using the finite element flow model (EFLOW) to simulate multi-level slug tests. EFLOW may be utilized to solve two dimensional flow in an axisymmetric domain using the Galerkin method. EFLOW was modified to accommodate transient hydraulic head and fluid flow conditions in the screened section. Using a modified form of EFLOW, slug tests were simulated for different well geometries for different screen positions relative to the nearest impermeable boundary. Slug tests were simulated for different degrees of anisotropy, storage coefficients, and radii of influence. Storage was determined to have a negligible effect on the dimensionless discharge after 1 second for storativity coefficients in the range of 0 to 10^{-4}. The storage effects were neglected by Widdowson et al. as the steady state region was judged to correspond to the log-linear portion of slug test recovery data. Given the negligible influence of storage, the method of Widdowson et al. would appear applicable to unconfined conditions as well. Widdowson et al. state that this method is only suitable for naturally developed wells where the screened section is fully submerged. Similar to the interpretation method of Dagan (1978), a family of curves of dimensionless discharge (P equal to Q' in Equation 19) versus $\log(L_s/R_s)$ was generated for a range of aquifer thickness to screen length ratios as shown in Figure 8. The slug test data analysis technique is identical to Dagan (1978), again using Equation 20. As stated by Widdowson et al., their technique may be viewed as an extension of Dagan's solution for small ratios of screen length to radius (L_s/R_s). A favorable comparison between the two methods was achieved for the zero storage, isotropic case for $L_s/R_s > 50$. The absolute difference between the two methods ranged from 0 to 4%, with the maximum difference occurring at $L_s/R_s = 50$.

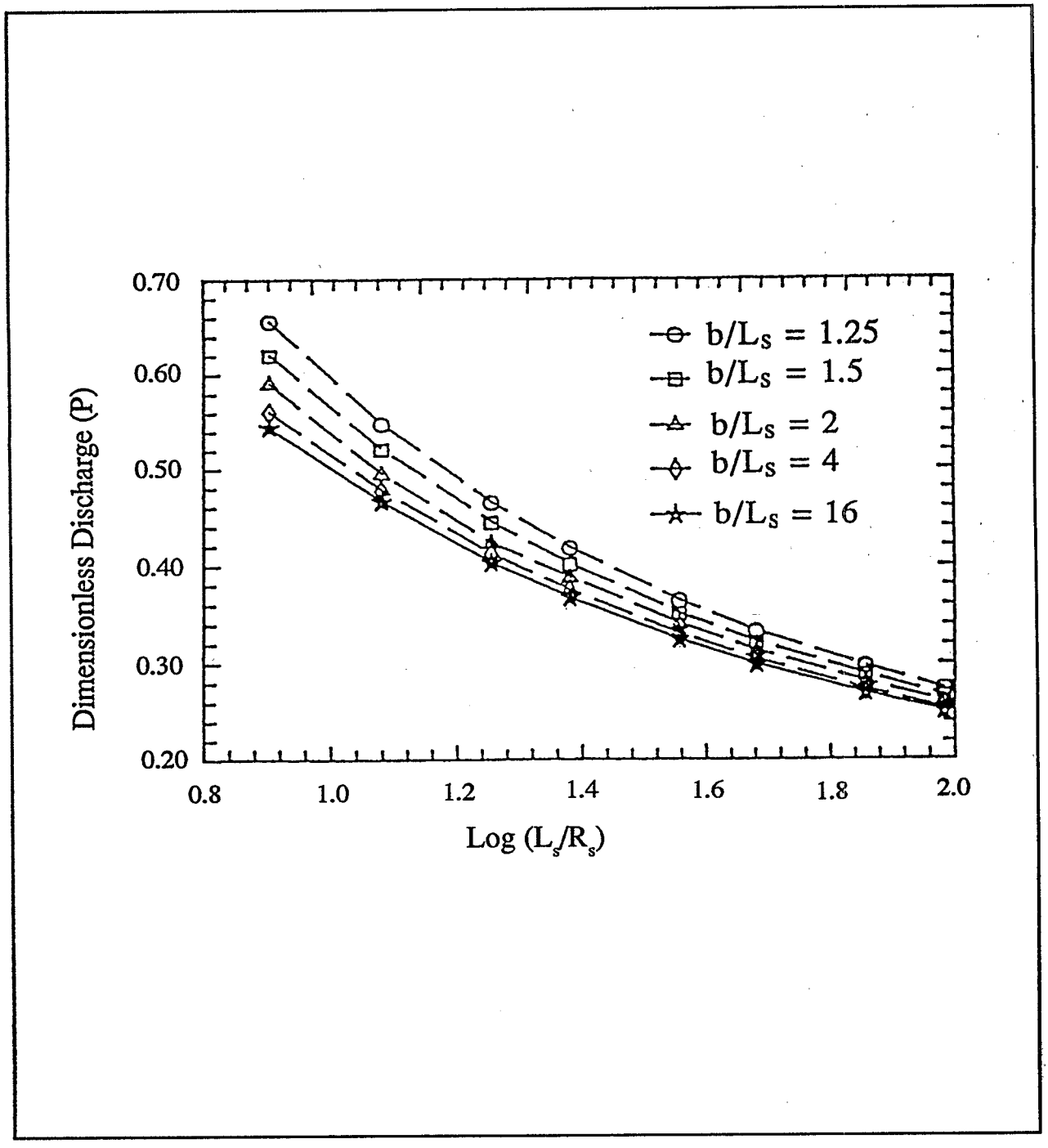

Figure 8. Variation in dimensionless discharge (P) for different degrees of partial penetration. b = aquifer thickness, R_s = well screen radius, and L_s = well screen length. After Widdowson et al., 1990.

SECTION 3

THEORETICAL ASSESSMENTS OF FACTORS AFFECTING SLUG TESTS

The analysis of slug tests may be adversely affected by borehole skin effects, anisotropy, determination of a radius of influence, partial penetration, approximation of intake shape factors, drainage of the filter pack in partially submerged screen wells, and poor curve matching. The potential effects of these factors on the calculated hydraulic conductivity value and methods for accounting for these factors is presented in this section. A new method is also presented to account for the drainage and re-saturation of the filter pack in wells with partially submerged well screens.

SHAPE FACTORS FOR THE 1/2 AND FULL ELLIPSE, AND DOUGHNUT MODELS

Shape factors constitute an unknown, or at least approximated, component of the solution to obtain hydraulic conductivity from slug tests in unconfined aquifers (Kirkham, 1946). In addition to the closed form analytical shape factors discussed in Chapter 2, shape factors have been approximated by electric analog and numerical methods. The analytical shape factors for the 1/2 ellipse (Equation 8) and the full ellipse (Equation 9), are compared as a function of the ratio of screen length to diameter ($L_s/2R_s$) in Figure 9. The $L_s/2R_s$ ratios for typical 5.08 cm (2 inch) diameter monitoring wells with 0.5, 1.0, 3.0 and 5.0 meter screens are 9.84, 19.69, 59.06, and 98.43, respectively. The difference between the two shape factors is small, increasing to a percentage difference of approximately 18% at the largest screen length to diameter ratio. Since the hydraulic conductivity is inversely proportional to the shape factor (see Equation 18), the difference between a calculated conductivity using either of these models would be relatively small.

Subsequent to the work of Kirkham (1946), additional shape factors for a cylindrical intake were obtained by 3-D electrical analog. Using a 3-D electrical analog in the laboratory, Frevert and Kirkham (1948) obtained values for the shape factor for the case when the soil is flush with the bottom of the casing. Luthin and Kirkham (1949) obtained values of the shape factor for the case of a 2.54 cm (1 inch) diameter cylindrical cavity open 1.27 to 10.16 cm below the end of the casing. Smiles and Young (1965) re-investigated these shape factors and found them to be consistently 12% too high. Smiles and Young attributed this to a constant erroneous measurement of the specific conductivity of the electrolyte. Smiles and Young (1965) also investigated the case of a hemi-spherical cavity below a casing, and provide a summary of previously determined shape factors.

The shape factor for a cylindrical intake has also been investigated by numerical methods. The earliest numerical shape factors were derived from finite difference methods (Wilkinson, 1968; Al-Dhahir and Morgenstern, 1969; Raymond and Azzouz, 1969). Al-Dhahir and Morgenstern (1969), for example, replaced the Laplace Equation in radial coordinates by a finite difference form and solved the resulting set of simultaneous linear

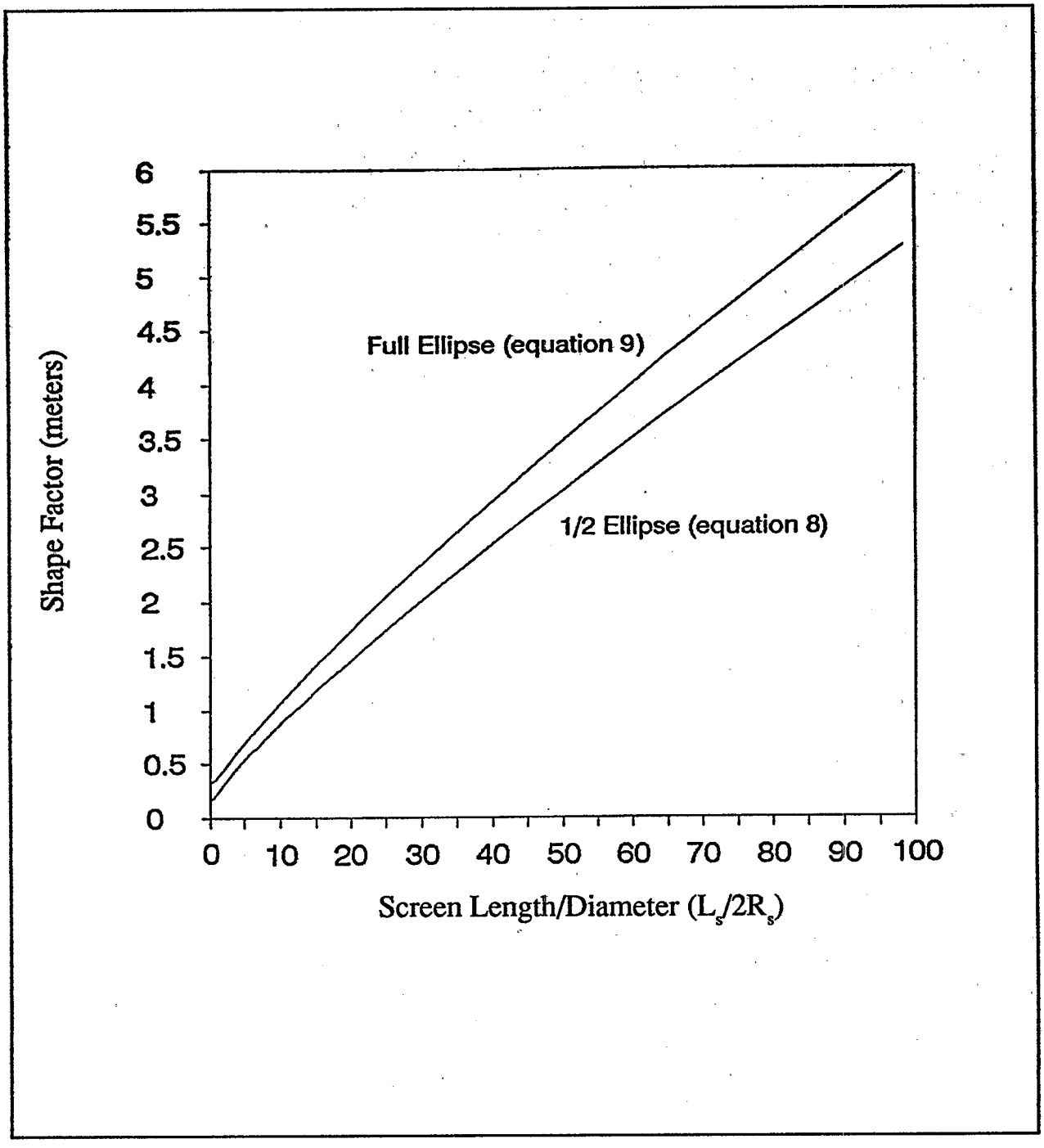

Figure 9. Comparison of analytical shape factors for the 1/2 and full ellipse models for 2.54 cm (1 inch) radius well screen and screen lengths ranging from 0.01 to 5 meters.

equations by an iterative method. Potential problems with these methods include adjustments required to solve convergence and the discontinuity problems in the corners of the physical domains where the method was applied (Chapuis, 1989). Shape factors have also been derived by finite element methods (Randolph and Booker, 1982: Tavenas et al., 1986a, 1986b). According to Chapuis (1989), these methods are known to have limited accuracy because conventional finite elements with nodes at their apexes do not insure continuity of both pore pressures and flow rates.

A comparison of the shape factors for cylindrical injection zones in an aquifer of infinite extent as proposed by the above authors is presented as a function of $L_s/2R_s$ in Figure 10 (after Chapuis, 1989). The majority of the shape factors fall into a narrow range with increasing divergence with increasing screen length to diameter ratios. The maximum percent difference among the shape factors shown in Figure 10 is approximately 40% (or a factor of less than 2) for $L_s/2R_s$ equal to 16, excluding the results of Randolph and Booker (1982). This percent difference remains approximately the same if the curves are linearly extrapolated to a typical monitoring well $L_s/2R_s$ ratio of approximately 59 (3 m screen length and 5.08 cm screen diameter). As such, it appears that the choice of a particular shape factors is not a major source of error in calculating hydraulic conductivity values. Recall that the hydraulic conductivity is inversely proportional to the shape factor.

Chapuis (1989) attributes the main differences in shape factors for cylindrical intake zones to the limitations of numerical methods, whether the shape factors incorporate either a pervious or impervious bottom, and the finite domains used in numerical methods. For cylindrical cavities with a pervious bottom, Chapuis (1989) recommends the use of Equation 9 for $L_s/2R_s > 1$. If the bottom of the cylindrical intake is impervious, Chapuis recommends subtracting $5.5R_s$ from the shape factor calculated using Equation 9, based on electric analog methods from Taylor et al. (1948). This method is approximately equivalent to subtracting the circumference of the bottom of the intake ($2\pi R_s$).

RADIUS OF INFLUENCE

Determination of the radius of influence of a slug test is needed to solve for hydraulic conductivity using the doughnut model and to estimate the volume of aquifer affected by a slug test. The radial distance influenced by the test is also related to the degree of well skin effects (Chapter 3.3) and to the influence of boundary conditions (Chapter 3.5).

Determination of the radius of influence depends on how it is defined. The radius of influence has been defined as the distance to the source of supply (Hvorslev, 1951), the radial distance over which the initial head drop is dissipated (Bouwer and Rice, 1976), as unbounded storage at some radial distance (Chirlin, 1989), and as the distance at which some fraction of the initial head drop occurs (Barker and Black, 1983). Sageev (1986) suggests that the practical radius of influence is the detectable radius of investigation and should be set according to the accuracy of the pressure or head recording devices used to detect it. From a

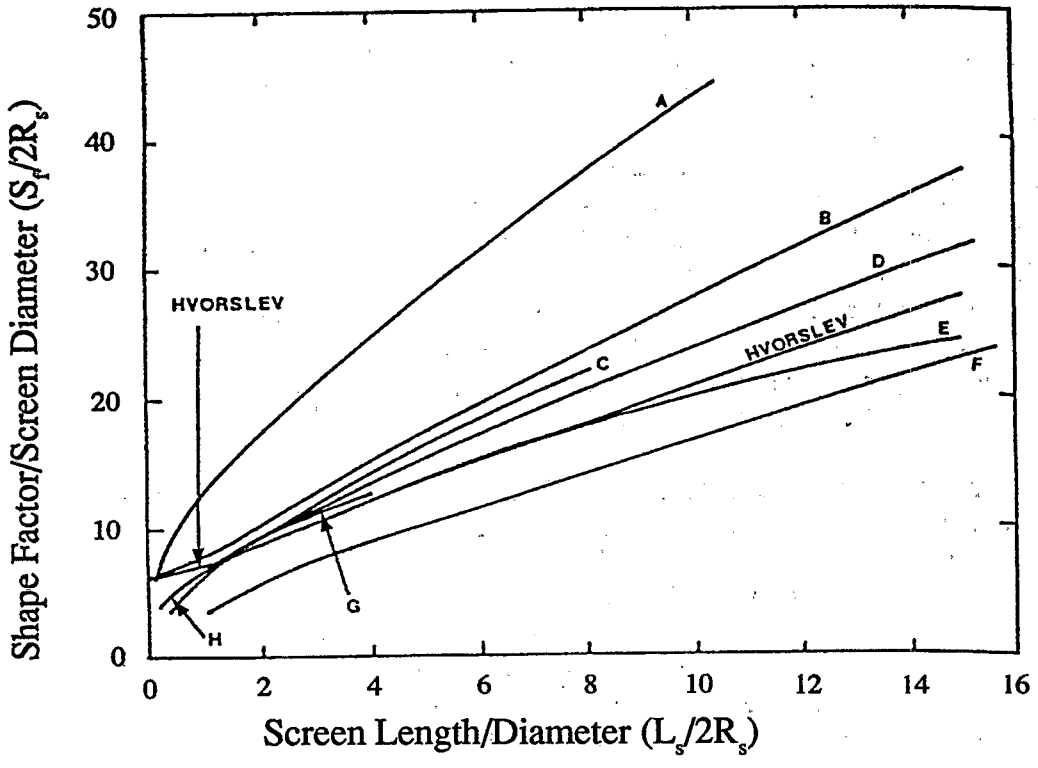

Figure 10. Comparison of analytical, electric analog, and numerical shape factors (normalized to the screen diameter) for cylindrical intakes. A = Randolph and Booker, 1982; B = Wilkinson, 1968; C = Tavenas et al., 1968a; D = Brand and Premchitt, 1980; E = Kallstenius and Wallgren, 1956; F = Raymond and Azzouz, 1969; G = Al-Dhahir and Morgenstern, 1969; H = Smiles and Young, 1956. After Chapuis, 1989.

mass balance perspective, a slug of water removed from a well will be replaced by an equal volume of water from the aquifer around the well. This volume in turn will be replaced by a subsequent volume of water coming from a radial distance further from the well. Assuming no storage and an infinite aquifer, mass balance implies that this replacement process must continue to infinity. While the radius of influence may be theoretically infinite, the actual radius of influence of a slug test is most likely finite due to storage or boundary effects.

The volume of aquifer which contributes to the recharge of a well is dependent on the volume of water removed from the well, the hydraulic conductivity of the aquifer, the screen length contributing to flow, aquifer storage, and boundary conditions. Larger head drops created in a well imply that larger volumes of the aquifer are affected. For the same head drop, a well with a longer screen would have a smaller radius of influence than one with a shorter screen. This is a consequence of water entering the well over a thicker portion of the aquifer. In addition, the radius of influence would decrease as the storage coefficient of the aquifer increases. Larger amounts of water are released from storage as the storage coefficient increases. If low permeable boundaries restrict vertical flow near the well, the radius of influence would increase relative to a homogeneous, isotropic aquifer of infinite extent. The same effect would occur if the aquifer is highly anisotropic, such that the horizontal conductivity is greater than the vertical conductivity. The Theis (1935) Equation for flow to a pumping well predicts a steep cone of depression diminishing rapidly away from a well in a low conductivity formation. Similarly, a slug test in a formation of low hydraulic conductivity would also affect a relatively small volume of aquifer.

The radius of influence appears in the shape factor for the doughnut model (see Equation 13). The shape factor decreases exponentially as the radius of influence increases. This can be seen in Figure 11 for a 5.08 cm diameter well with a 0.2, 0.5, 1.5 and 3.0 meter screen section using an arbitrary range of 0 to 30 meters for radii of influence. Reference to Equation 18 indicates that a reduction in the shape factor would increase the resulting hydraulic conductivity value, i.e., the larger the radius of influence the larger the hydraulic conductivity. The shape factor is very sensitive at radii of influence less than approximately 2 meters and appears to approach the screen length in the limit.

Bouwer and Rice (1976) investigated the radius of influence using a 2-D electrical resistance network analog for different well and aquifer geometries. The radial extent of the analog was 60,000 times the largest screen radius used in the analyses. Current flow to a 'well' for varied well and aquifer geometries was converted to volumetric flow (Q). Values of $\ln(R_e/R_s)$ were calculated from a modified Thiem Equation for steady state flow at given values of constant head (H):

$$Q = 2\pi K L_s \frac{H}{\ln(R_e/R_s)} \qquad (28)$$

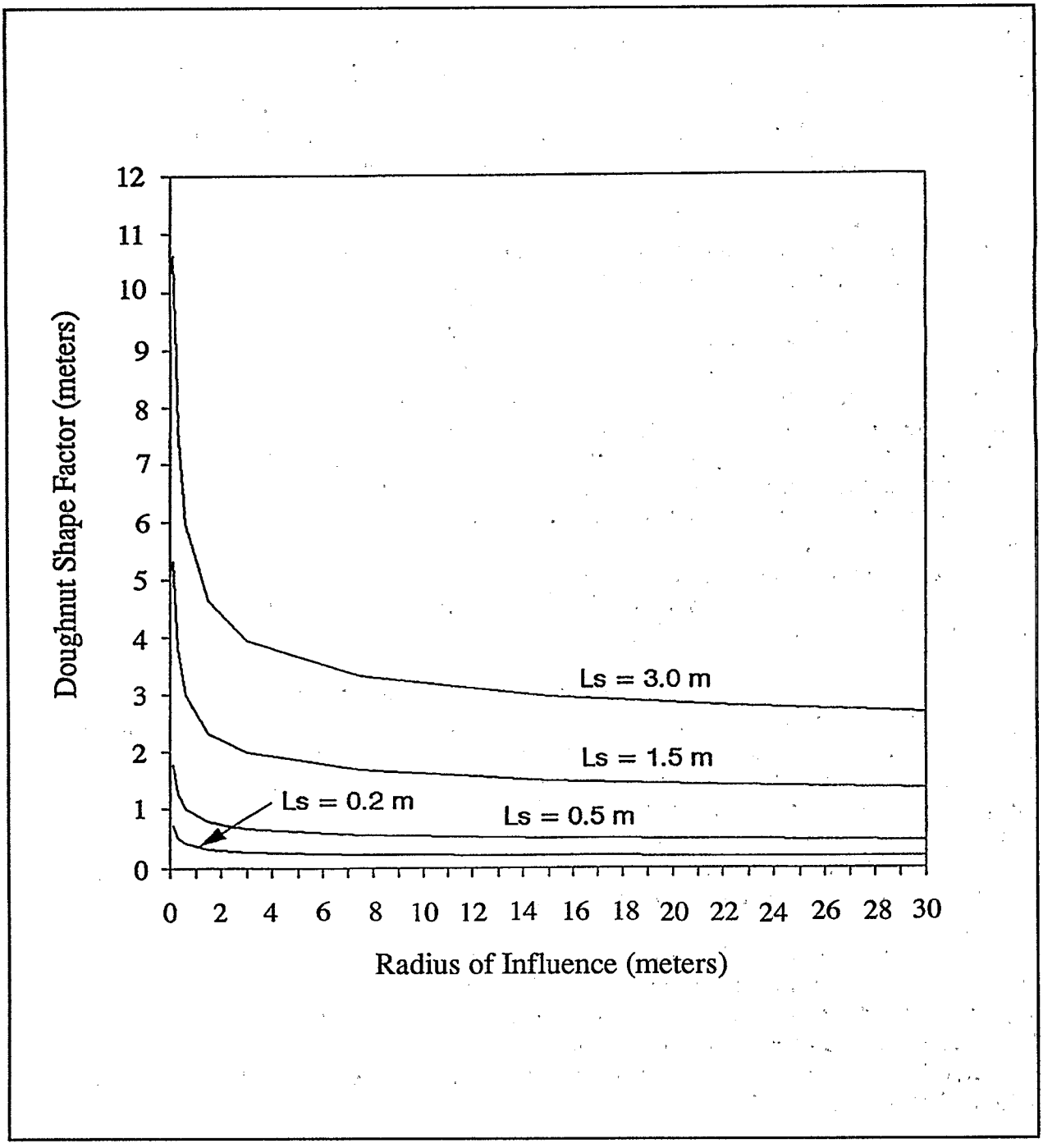

Figure 11. Impact of the radius of influence and screen length (L_s) on the doughnut model shape factor for a 2.54 cm radius well screen.

The test geometry is illustrated in Figure 12. Different values of the radius of influence, as $\ln(R_i/R_s)$, were determined for different sets of aquifer thickness, screen radius, and position of the bottom of the screen relative to both the water table (L_w-L_s) and the lower confining unit (b-L_w = D'). The position of the top of the screen immediately at the water table was not evaluated directly, as a short between the water table as a source and the well as a sink would have occurred. Current flow to the well was found to vary linearly with screen length. This allowed extrapolation for the case where the top of the screen was at the water table. Based on the results of the electric analog work, empirical formula were derived for $\ln(R_i/R_s)$ for the case of fully and partially penetrating well screens, presented here as Equations 29 and 30, respectively:

$$\ln\left(\frac{R_i}{R_s}\right) = \left(\frac{1.1}{\ln(L_s/R_s)} + \frac{A + B\ln((b-L_w)/R_s)}{(L_s/R_s)}\right)^{-1} \tag{29}$$

$$\ln\left(\frac{R_i}{R_s}\right) = \left(\frac{1.1}{\ln(L_s/R_s)} + \frac{C}{(L_s/R_s)}\right)^{-1} \tag{30}$$

The terms A, B, and C are empirical constants. These constants are a function of (L_s/R_s) and can be selected graphically from Figure 13 (after Bouwer and Rice, 1976). Bouwer and Rice (1976) report increasing error as the screen length decreased relative to the steady state head. They report 10% error for $L_s > 0.4H$, and 25% error if $L_s << H$. For one case, the calculated radius of influence was compared to the equipotential lines radiating from the electric analog of the well. The calculated radius of influence corresponded to equipotential lines representing 85% of the initial head drop in the horizontal and 80% in the vertical directions. They concluded that this radius is indicative of the portion of the aquifer sampled for hydraulic conductivity from slug tests. The method of Bouwer and Rice for determination of R_i is only 2 dimensional and only for steady state conditions. Additional error may result from having to read empirical constants from a graph, the discrete nature of their network, and imperfect calibration of the individual resistance elements in their model (Dagan, 1978). The Bouwer and Rice method for calculating the radius of influence is also independent of the hydraulic conductivity and specific yield of the aquifer, as well as the initial head drop created by the slug test.

The Bouwer and Rice method was applied here to typical monitoring well geometries in order to estimate radii of influence. The radii of influence for two fully penetrating wells with screen radii of 2.54 cm (typical casing radius) and 11.43 cm (typical hole radius) was calculated using Equation 30 for variable screen lengths ranging from 1 to 10 meters. The results are presented in Figure 14. The radius of influence was found to range from 0.27 to 2.65 meters, and from 0.37 to 3.35 meters for the 2.54 and 11.43 cm radii well screens, respectively. The radius of influence was found to increase linearly with screen length with a correlation coefficient of 0.999 for both well screen radii. The direct correlation between

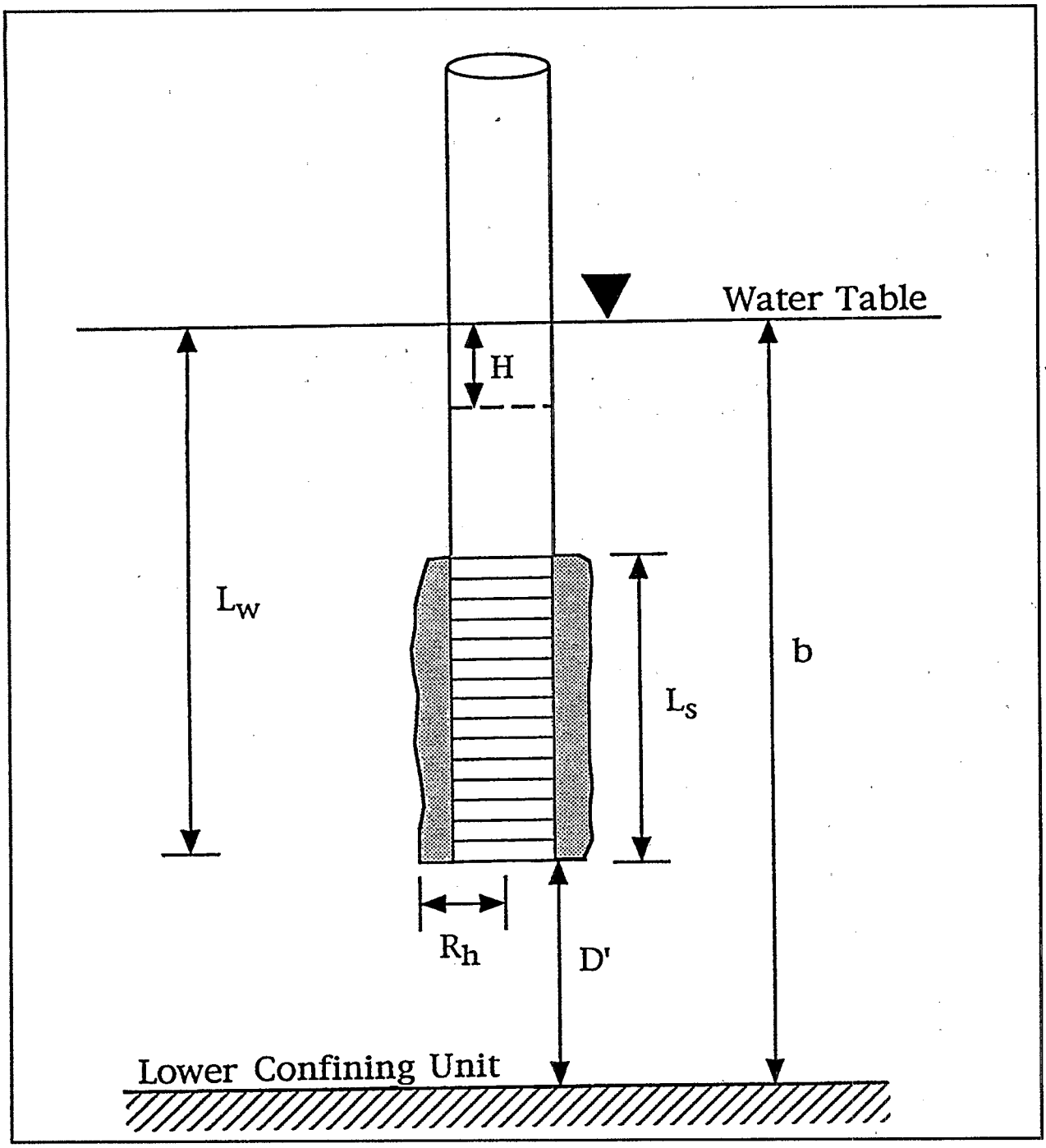

Figure 12. Well and aquifer geometry symbols for the Bouwer and Rice (1976) model.

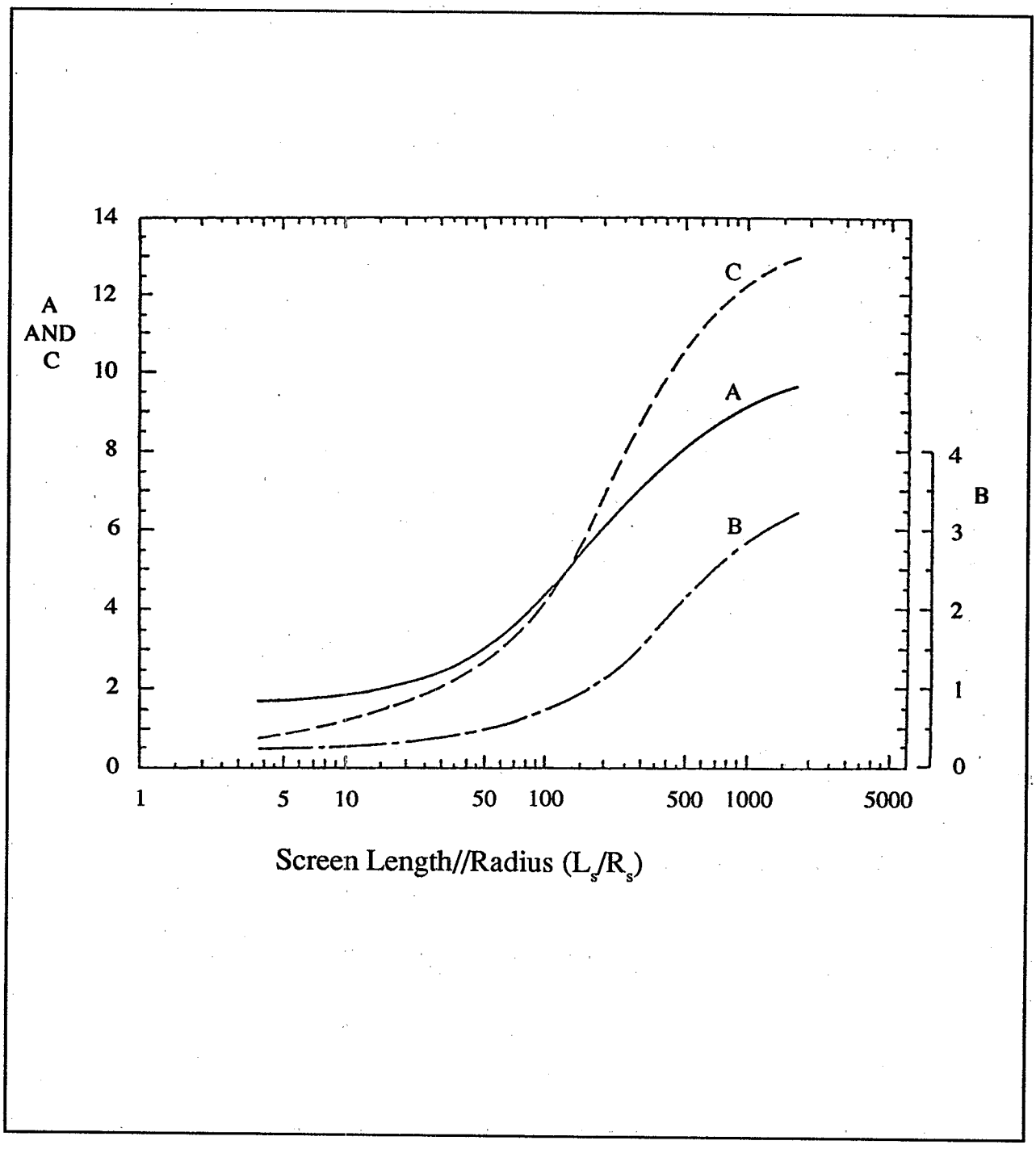

Figure 13. Dimensionless parameters A, B, and C for the Bouwer and Rice (1976) model.

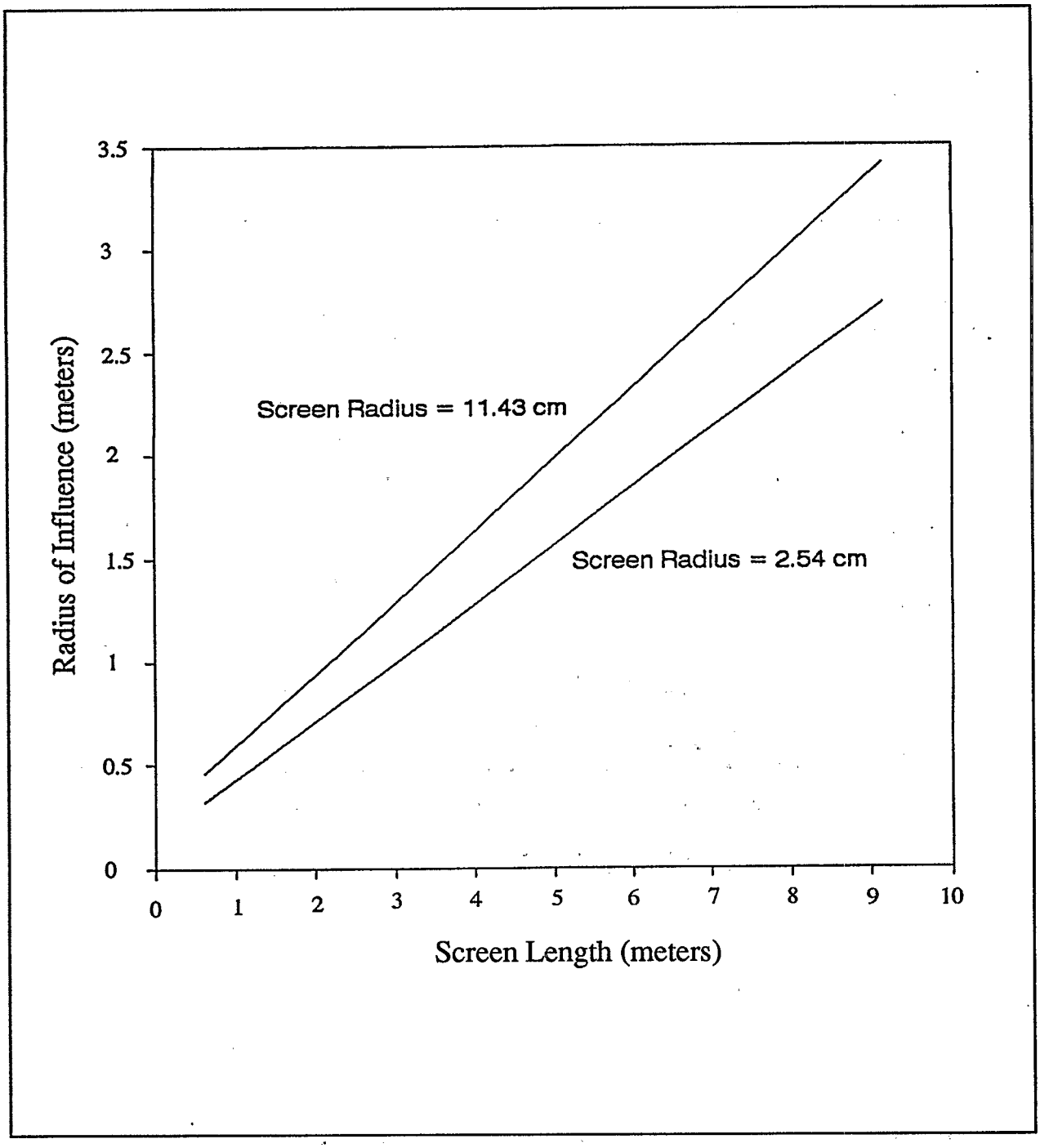

Figure 14. Impact of screen length and screen radius on the radius of influence, calculated using the Bouwer and Rice (1976) method.

screen length and radii of influence is a consequence of having wells that are fully penetrating and having radial flow. The radius of influence was found to be approximately one third the screen length.

The screen length variable (L_s) in the full ellipse model and the radius of influence variable (R_i) in the doughnut model are present in the terms $\ln(L_s/R_s)$ and $\ln(R_i/R_s)$, respectively, as presented in Equations 11 and 12. Differences between hydraulic conductivity values calculated using the two models are only a function of the difference between these two terms. The presence of the natural log function in each of the terms will further reduce the difference between the two methods. The doughnut model shape factor was calculated using Equation 13, incorporating the radius of influence calculated using Equation 30 for a fully penetrating 2.54 cm radius well with a screen length ranging from 1 to 10 meters. The full ellipse model shape factor was calculated for the same well geometry using Equation 9. Figure 15 is a comparison of the two shape factors. Shape factors derived from the doughnut model were consistently higher and increased with screen length at a faster rate than the full ellipse model. However, the percent difference between the two shape factors increased linearly from only 3.95% for a 0.61 meter screen to 32% for a 9.14 meter screen. Hence, hydraulic conductivity values determined using either model will not be significantly different, especially at smaller screen length to diameter ratios.

Widdowson et al. (1990) using the modified form of EFLOW found that setting the radius of influence between 18.29 and 182.88 meters (60 to 600 feet) resulted in 2% to 5% difference in the resulting dimensionless discharge (P) from numerically simulated slug tests. Widdowson et al. held the value of R_i constant for generation of dimensionless discharge values for given well geometries. They found that the dimensionless discharge term is equivalent to the inverse of the $\ln(R_i/R_s)$ term of the doughnut model. Therefore, calculation of hydraulic conductivity values using the Widdowson et al. method will yield approximately the same value as the Bouwer and Rice method for isotropic conditions far from an impermeable boundary.

Determination of a representative radius of influence may also be approached from a mass balance performed on the volume of the slug of water removed from a well. Assuming that no water is released from storage, the volume of water removed from the well (V_o) must be replaced by an equal volume of water (V_1) extending from the well screen to a radial distance R_1. This volume must be similarly replaced by volume V_2 extending to a radial distance R_2. The equations for the volumes of each replacing cylinder follow as Equations 31-34, and are shown in generic form for any volume, V_n, in Equation 35. In the following equations, n equals the formation porosity. Note that any incremental volume must be equal to the original volume of water added or removed from the well (Equation 36).

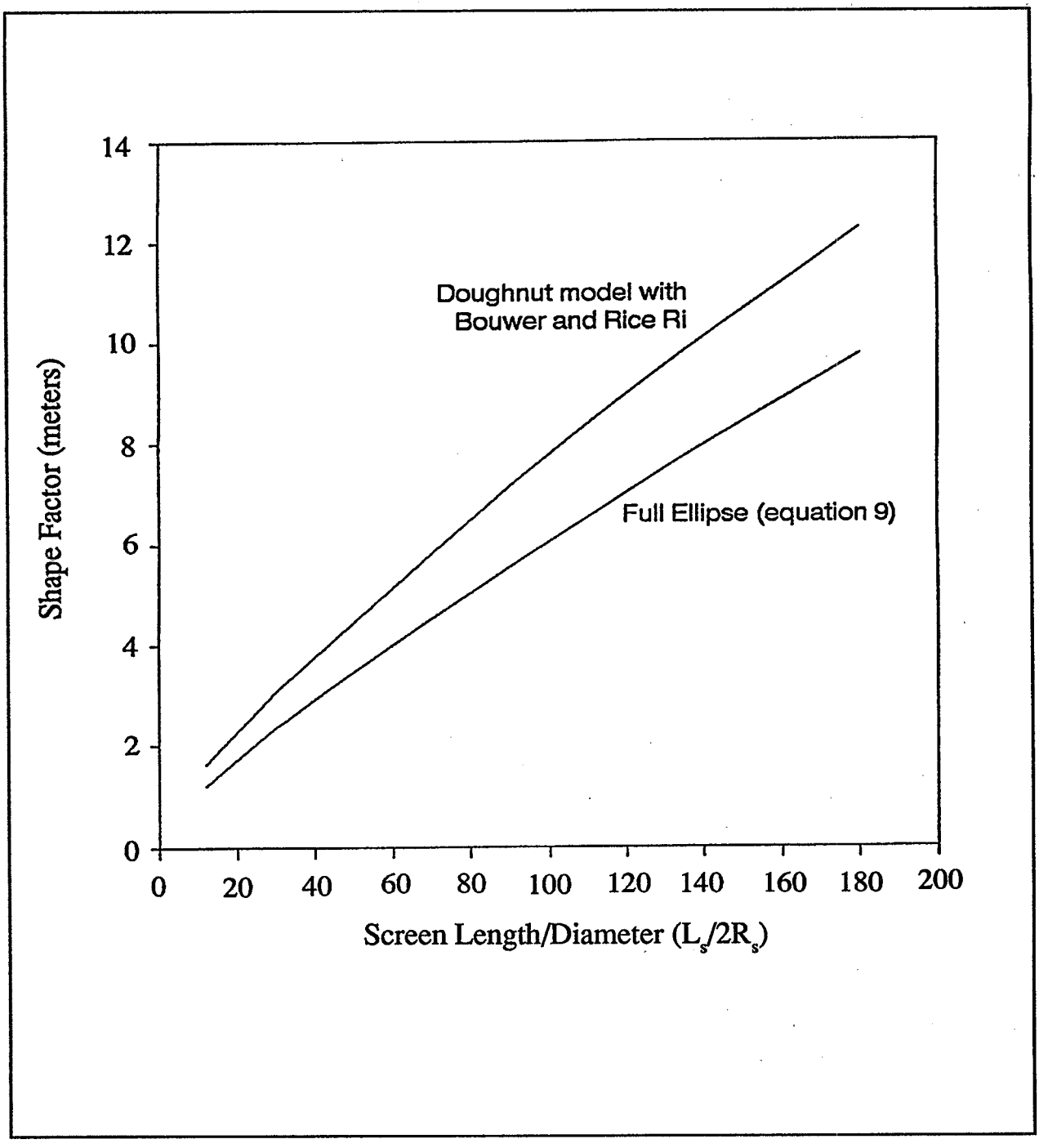

Figure 15. Comparison of shape factors for the doughnut model using Bouwer and Rice (1976) radii of influence, and for the full ellipse model for a 2.54 cm radius well screen.

$$V_1 = \pi R_1^2 L_s n - V_o = \pi R_1^2 L_s n - \pi R_c^2 H_o \quad (31)$$

$$V_2 = \pi R_2^2 L_s n - V_1 - V_o = \pi R_2^2 L_s n - \pi R_1^2 L_s n + \pi R_c^2 H_o \quad (32)$$

$$V_3 = \pi R_3^2 L_s n - V_2 - V_1 - V_o = \pi R_3^2 L_s n - \pi R_2^2 L_s n + \pi R_1^2 L_s n - \pi R_1^2 L_s n + \pi R_c^2 H_o - \pi R_c^2 H_o \quad (33)$$

$$V_3 = \pi R_3^2 L_s n - \pi R_2^2 L_s n \quad (34)$$

$$V_n = \pi R_n^2 L_s n - \pi R_{n-1}^2 L_s n \quad (35)$$

$$\pi R_c^2 H_o = \pi R_n^2 L_s n - \pi R_{n-1}^2 L_s n \quad (36)$$

While the replacing volumes must remain equal, the incremental increase in radial distance will decrease with each additional replaced volume. The radius of influence of a slug test may then be regarded as the distance at which the percent difference between the increasing radial distances becomes negligible. Dividing through by π, and rearranging Equation 36 allows for setting the percent difference between two adjacent radial distances.

$$R_n^2 - R_{n-1}^2 = R_c^2 H_o / L_s n \quad (37)$$

Selection of a limit for the percent difference between the increasing radial distances is arbitrary. If the percent increase in radial distance is only 1%, then R_{n-1} is equivalent to $0.99R_n$, and R_n becomes the radius of influence.

$$R_n^2 - (.99R_n)^2 = R_c^2 H_o / L_s n \quad (38)$$

x

$$R_n = R_i = \sqrt{\frac{50.25(R_c^2)H_o}{L_s n}} \quad (39)$$

If the difference between the two radii is selected as 0.1% or 10%, the resultant equations for calculation of the radius of influence would be Equations 40 and 41 respectively.

x

$$R_n = R_i = \sqrt{\frac{5.26(R_c^2)H_o}{L_s n}} \quad (40)$$

x

$$R_n = R_i = \sqrt{\frac{500.25(R_c^2)H_o}{L_s n}} \quad (41)$$

Examination of the above equations indicates that the radius of influence is proportional to the volume of water removed from the casing, and inversely proportional to both the screen length and the porosity. Using the above equations, with an initial drawdown equal to the screen length and a porosity of 30%, yields a radius of influence equal to $40.84R_c$, $12.94R_c$ and $4.15R_c$ for a 0.1, 1.0 and 10% difference in increasing radii, respectively. For a typical 5.08 cm diameter well casing, these values correspond to radii of influence of 1.04, 0.33, and 0.11 meters, respectively, from the well screen. This range is significantly less than those calculated by the Bouwer and Rice method for a fully penetrating well. These calculations further support that a slug test only influences a small volume of aquifer and emphasizes the need to carefully construct and develop wells for slug testing to minimize adverse factors such as well skin effects, clogged screens, and formation disturbance.

WELL SKIN EFFECTS

The process of well drilling, emplacement of a filter pack around the screen, penetration of drilling mud into the formation, and the well development process may produce a disturbed zone around a well commonly referred to as a well skin. Well skins may be more permeable than the formation, e.g., a high permeability filter pack around the screen section; or less permeable than the formation, e.g., borehole damage due to smearing of clays or other fines along the borehole. More permeable well skins would increase the apparent hydraulic conductivity as determined from a slug test, and a less permeable well skin would have the opposite effect. The impact of well skin effects on slug tests may be considerable, especially if the disturbed zone is large relative to the volume of aquifer tested by the slug test.

Kipp (1985) describes the skin effect as an empirical concept based on postulating an additional pressure drop through a thin annulus around the well bore that is proportional to the flow rate into the well. Van Everdingen (1953) discussed the effects that well bore skin have on the pressure response of a well for the case of constant discharge. Jaeger (1956) considered the solution to a heat flow slug test that included well bore storage and skin. The skin effect was also described by Carslaw and Jaeger (1960). The analytical solution for a slug test in a well surrounded by an infinitesimally thin skin was originally published by Ramey and Agarwal (1972), and updated by reducing the number of dimensionless parameters by Ramey et al. (1975). Faust and Mercer (1984) presented a ignite difference model of a slug test response in a well having a finite skin thickness. Moench and Hsieh (1985) contend that the results of Ramey and Agarwal (1972) and Faust and Mercer (1984) are actually identical. A finite element solution for quasi-steady state flow to a double packer system was presented by Braester and Thunvik (1984) which included an evaluation of the effects of well skin and anisotropy. The effects of well skin, as well as anisotropy, boundaries and partial penetration, was also considered by McElwee et al. (1990).

Faust and Mercer (1984) numerically simulated four slug test runs with a well skin hydraulic conductivity of 0.01, 0.1, 1.0, and 10 times the hydraulic conductivity of the formation. For their simulations, the well radius was 0.385 m, the casing radius was 0.0205 m, the initial head was 5.0 m, and the storativity was 2.25×10^{-8}. The thickness of the well

skin was equivalent to the radius of the borehole. Their results for a formation having a hydraulic conductivity of 10^{-9} are presented in Figure 16. The Figure indicates that a more permeable well skin has little effect on the position or shape of the recovery curve. Hence, their results suggest that a more permeable well skin would have little effect on the calculated hydraulic conductivity. However, less permeable well skins significantly influenced the recovery curves. Using the type curve method of Cooper (1967), this would lead to underestimating the formation's hydraulic conductivity. The similar shape of the curves would not indicate the presence of a well skin. Moench and Hsieh (1985) indicate that the hydraulic head response in a slug test interval may respond to the skin properties at early time and to aquifer properties at late time. Moench and Hsieh suggest that Faust and Mercer would have found the same results, if they considered a typical aquifer with storativity values in the range of 10^{-3} to 10^{-6}.

Braester and Thunvik (1984), using a finite element model, evaluated the effect of well skin on steady state flow to packer tests using input parameters reproduced from a series of tests on a granite. The input parameters include a porosity of 0.3%, total water and rock compressibility of 10^{-10} Pa^{-1}, borehole radius of 0.028 m, a packer spacing of 2 m, and an injection overpressure of 4×10^5 Pa. Their numerical results compared well with the full ellipse model (Equation 11), Dagan's (1978) analytical solution to the double packer flow, and with Moye (1967) as shown in Figure 17. The maximum relative difference between the numerical results and Dagan's formula was 4% at the smallest ratio of well screen length to radius ratio examined ($\log (L_s/R_s) = 1.85$). The maximum relative difference between the results of the full ellipse and Moye's formula with those of Dagan's was 8.8 and 14.6%, respectively, also at $\log (L_s/R_s) = 1.85$. To evaluate the effect of borehole skin, apparent permeability values were numerically computed for skin radii ranging from 0.11 to 0.33 m from a 0.028 m radius borehole. The skin permeability values used were 0.001, 0.01, and 0.1 times the intrinsic permeability of the formation (10^{-12} m^2). The numerically generated steady state flows were then used in Dagan's formula to evaluate the composite apparent permeability. Using the data tabulated in Braester and Thunvik (1984), a graph of the apparent permeability versus the well skin radius was generated as Figure 18. As shown on the Figure, the apparent permeability closely mimics the well skin permeability. The case of a more permeable well skin was not investigated.

McElwee et al. (1990) investigated the effects of well skin in both a fully penetrating and partially penetrating well in an isotropic medium. They used an analytical solution obtained in Fourier-Laplace space and inverted for a solution in space-time domain using the Stehfest algorithm for a numerical approximation of the inversion. McElwee et al. indicate that for a fully penetrating well with no skin, their solution is identical to Cooper et al. (1967). For the isotropic case with well skin, their solution reduces to the Laplace-space solution of Moench and Hsieh (1985). Simulations were conducted for the case of a fully penetrating well, with a skin radius 10 times the well radius and a skin hydraulic conductivity two orders of magnitude greater and less than the formation. As shown in Figure 19, their results also indicate that a less permeable well skin has a far greater impact than the more permeable well skin. The more permeable well skin, however, did affect the curves. The case

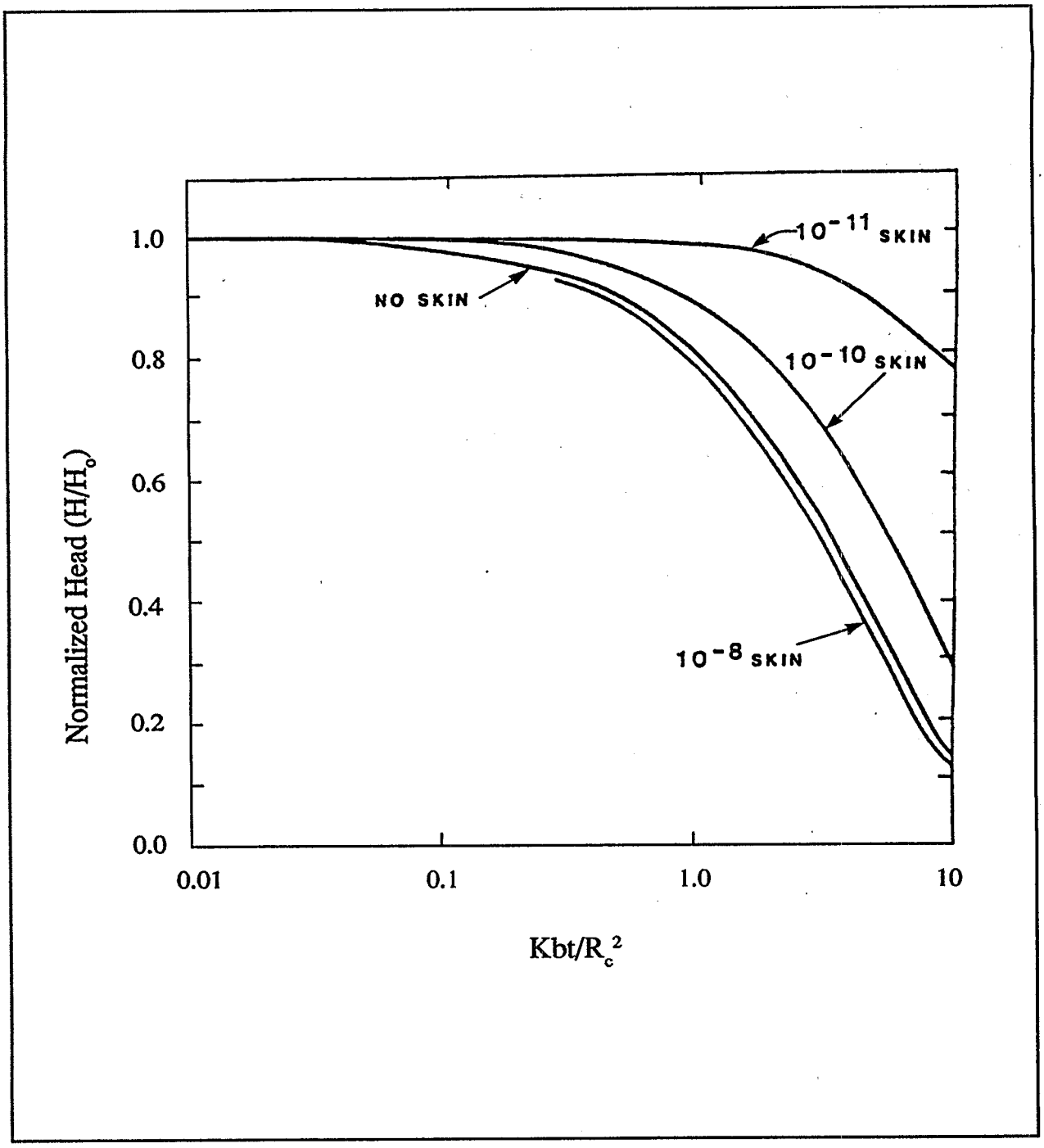

Figure 16. Recovery curves for varying skin hydraulic conductivities. Numbers adjacent to curves represent skin conductivities in m/s. K = formation hydraulic conductivity, b = aquifer thickness, t = time, R_c = well casing radius, and H/H_o = normalized head. After Faust and Mercer, 1984.

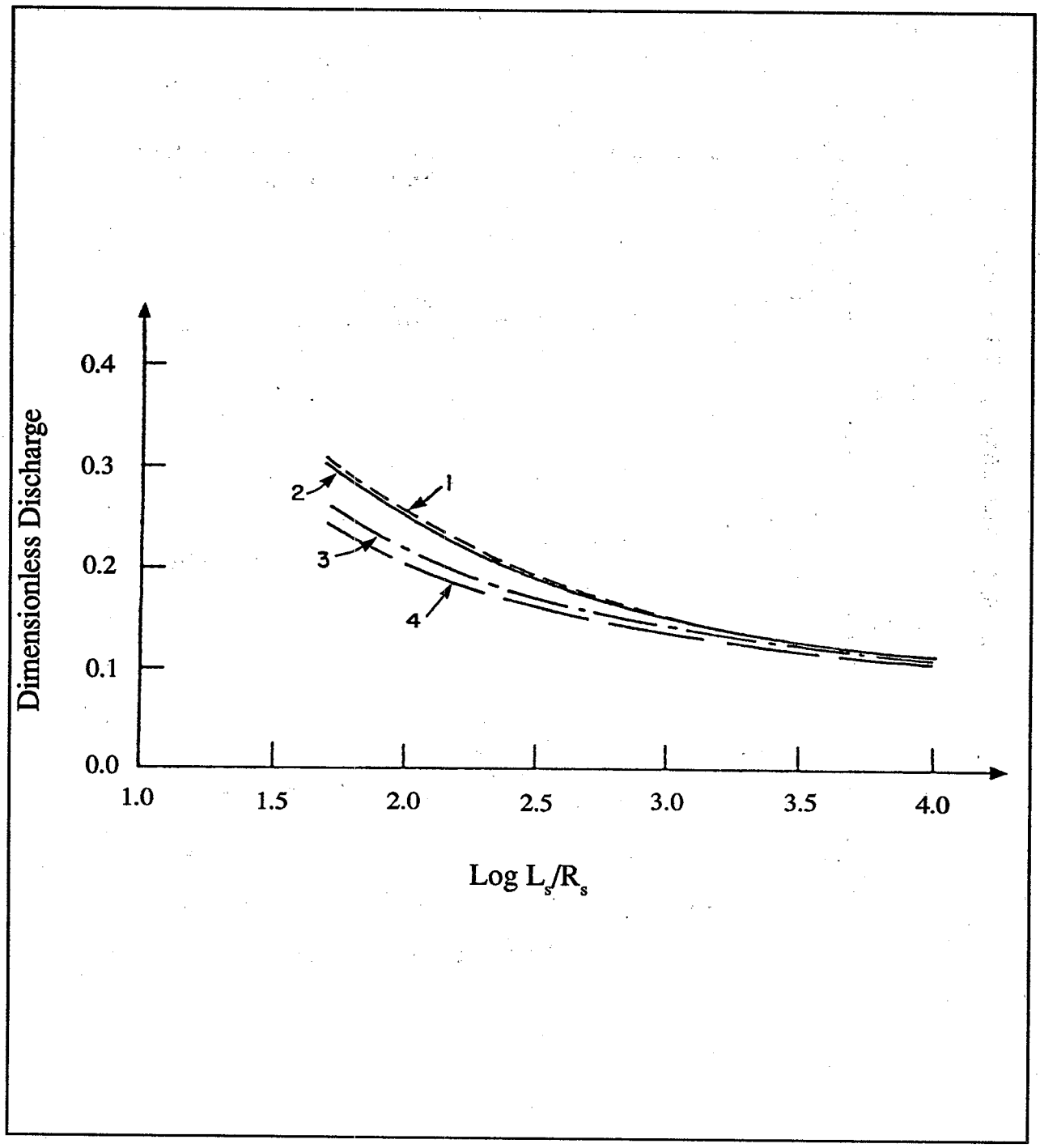

Figure 17. Comparison of cylindrical intake dimensionless discharge terms. (1) Braester and Thunvik's (1984) numerical solutions; (2) Dagan, 1978; (3) Hvorslev, 1951; and (4) Moye, 1967. L_s = well screen length; R_s = well screen radius. After Braester and Thunvik, 1984.

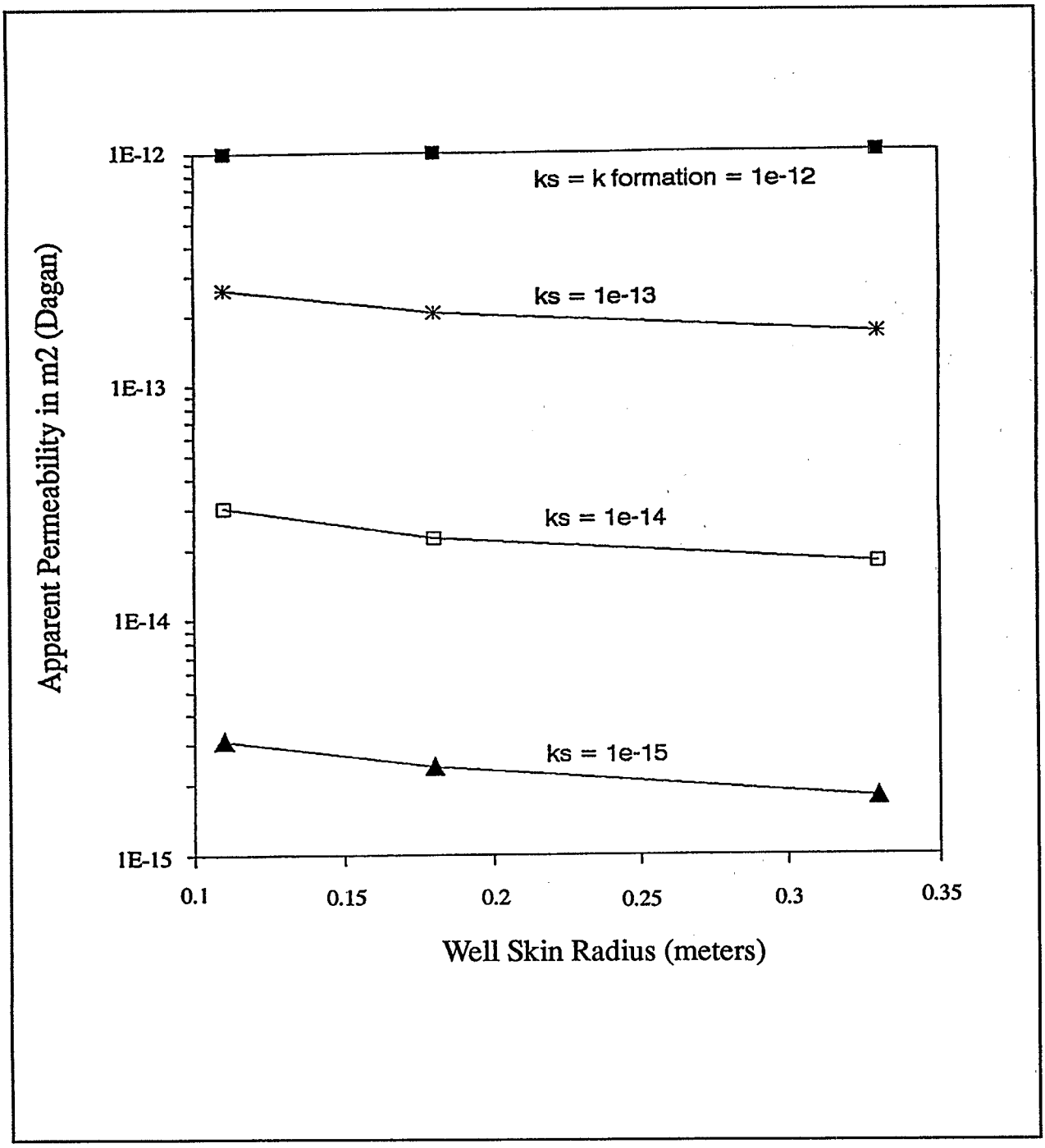

Figure 18. Apparent formation permeability for different well skin permeabilities (k_s) and thicknesses, using data from Braester and Thunvik, 1984.

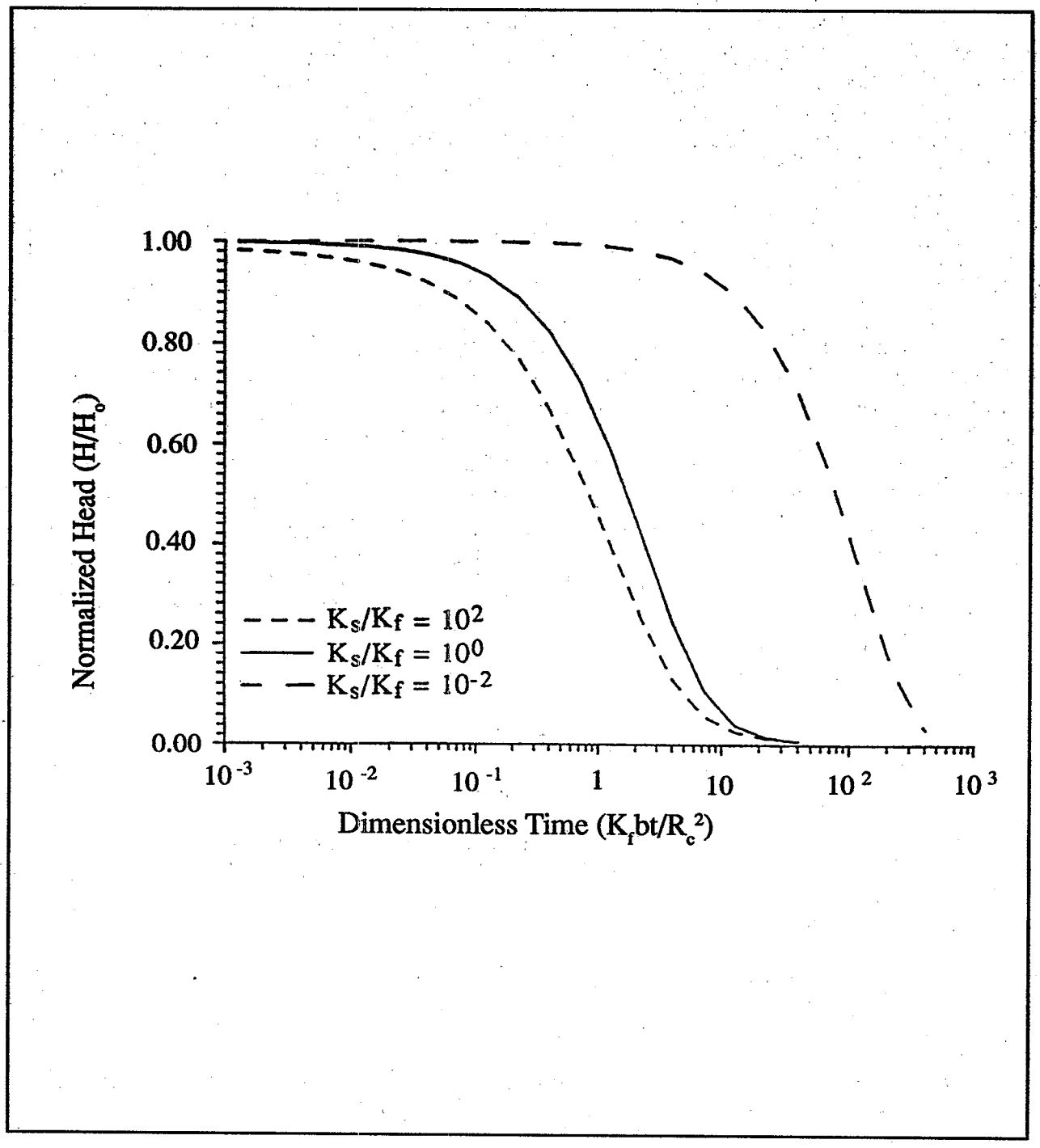

Figure 19. Effects of borehole skin on recovery curves for a fully penetrating well in a confined aquifer. K_s and K_f are the skin and formation conductivities, respectively. After McElwee et al., 1990.

of the partially penetrating well appears to have still included a fully penetrating well skin. The effect of the more permeable skin in this case was accentuated due to a fully penetrating preferential pathway to the well screen.

The influence of a well skin on the hydraulic conductivity value determined from a slug test may also be treated using radial averaging. Recall the Thiem Equation for steady state radial flow:

$$Q = \frac{2bK(H_s-H_i)}{\ln(R_i/R_s)} \tag{42}$$

If a well skin is present, the determined hydraulic conductivity will be a composite of both the well skin and the formation, which may be considered as an effective hydraulic conductivity (K_{eff}). The total head drop in the system will be the same, with a portion of the head drop taken up in the well skin and a portion in the formation. The flow rate (Q_s) coming into the screen will be equivalent to the flow coming through the borehole or well skin (Q_h), which in turn will be equivalent to the flow coming through the formation (Q_f). The conservation of flow regime is depicted in Figure 20 for reference. Three steady state flow equations may therefore be written representing the composite flow through the entire system from the radius of influence to the screen (43), flow through the well skin to the screen (44), and flow through the formation to the well skin (45). Note that the radius of the well skin is given as the borehole radius, R_h. In the following equations, the subscripts s, h, f, i relate to the screen, borehole or well skin, formation, and radius of influence, respectively.

$$Q_s = \frac{2\pi bK_{eff}(H_i-H_s)}{\ln(R_i/R_s)} \tag{43}$$

$$Q_h = \frac{2\pi bK_s(H_h-H_s)}{\ln(R_h/R_s)} \tag{44}$$

$$Q_f = \frac{2\pi bK_f(H_i-H_h)}{\ln(R_i/R_h)} \tag{45}$$

As stated above, the total head drop across the system is equivalent to the head drop across the well skin plus the head drop across the formation:

$$(H_i-H_s) = (H_i-H_h) + (H_h-H_s) \tag{46}$$

Re-writing Equations 43, 44, and 45 into Equation 46 yields:

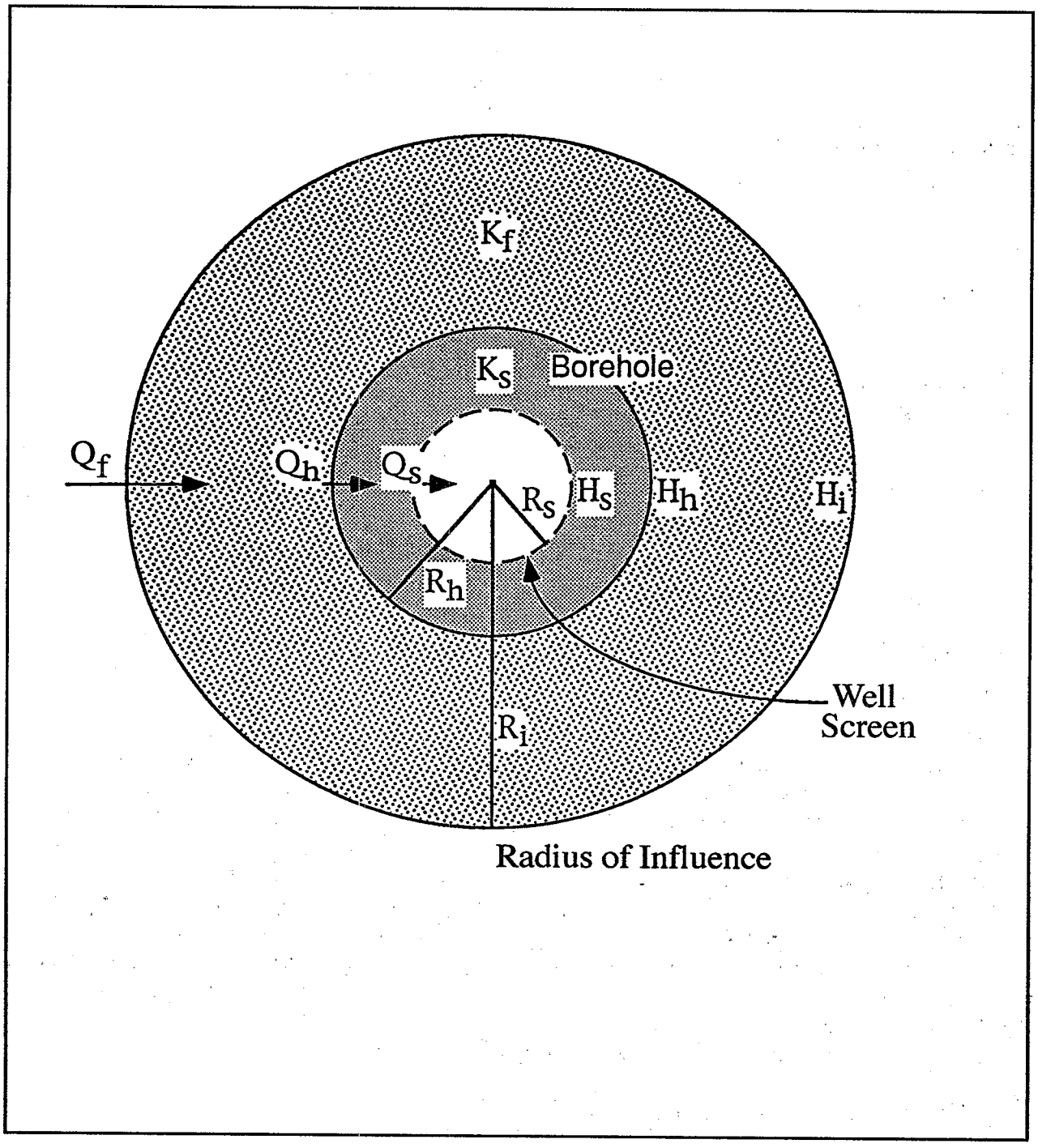

Figure 20. Plan view of a well identifying parameters used to derive effective hydraulic conductivity equation. Q, R, K, and H represent the flow, radius, hydraulic conductivity and hydraulic head at the labeled boundaries, respectively.

$$\frac{Q_s \ln(R_i/R_s)}{2\pi b K_{eff}} = \frac{Q_h \ln(R_h/R_s)}{2\pi b K_s} + \frac{Q_f \ln(R_i/R_h)}{2\pi b K_f} \quad (47)$$

Solving Equation 47 for K_{eff} yields:

$$K_{eff} = \frac{\ln(R_i/R_s)}{\frac{\ln(R_h/R_s)}{K_s} + \frac{\ln(R_i/R_h)}{K_f}} \quad (48)$$

Equation 48 may also be written as a ratio of the effective to formation hydraulic conductivity:

$$K_{eff}/K_f = \frac{\ln(R_i/R_s)}{\frac{\ln(R_h/R_s)}{K_f/K_s} + \ln(R_i/R_h)} \quad (49)$$

The effect of the radius of influence on the ratio of effective to formation conductivity was calculated using Equation 49, for a 2.54 cm radius well screen with either a 5.08 and 10.16 cm radius well skin. A K_s/K_f ratio equal to 10 and 0.1 was used. Results are shown in Figure 21. The Figure indicates that the conductivity will be overestimated in the case of a more permeable well skin, and underestimated for the case of a less permeable well skin. The maximum degree of over- or underestimation approaches the ratio of the skin to formation conductivity as the radius of influence diminishes. It should be noted that the maximum possible difference for the situation presented in Figure 21 is a factor of 10. As the radius of influence increases, the effective conductivity approaches the formation conductivity in an exponential manner. This occurs to a greater degree and more rapidly for the case of the well skin with a higher conductivity than the formation. The effect of a less permeable well skin is more pronounced and cannot be readily overcome by increasing the radius of influence (i.e., by increasing the initial head drop). A more permeable well skin will affect the results of a slug test, but with a radius of influence of less than one half of a meter, this effect may be reduced to less than a factor of 2.

ANISOTROPY AND HETEROGENEITIES

Most natural geologic formations have a strong horizontal to vertical anisotropy ratio with respect to hydraulic conductivity (Taylor et al., 1990). Anisotropy ratios of 10:1 or more are common (Freeze and Cherry, 1979). Formation heterogeneities due to natural layering may also be present. Measurements of hydraulic conductivity determined from slug tests may reflect these anisotropies, either under- or overestimating the hydraulic conductivity

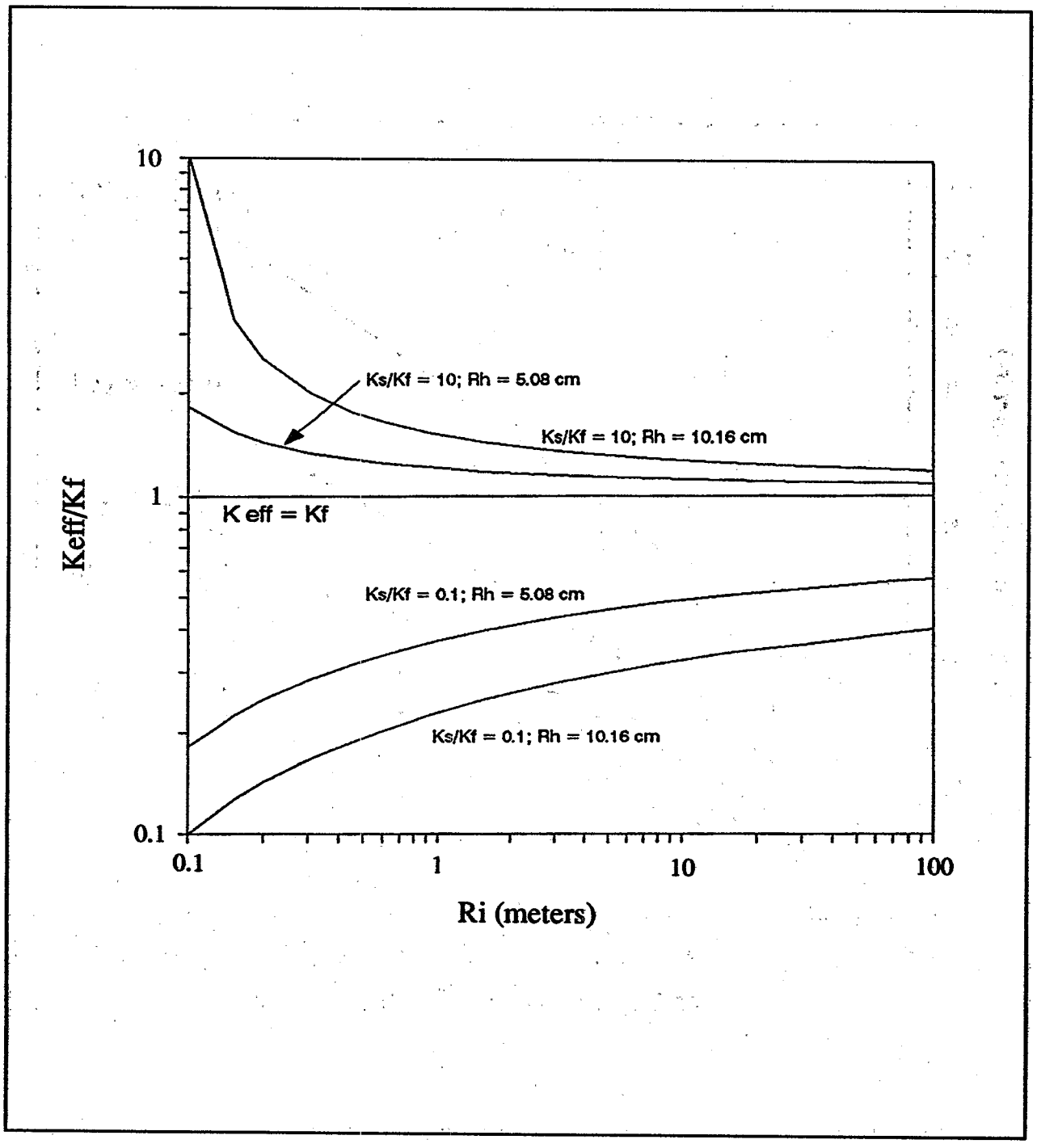

Figure 21. Effects of well skin and radius of influence on the effective hydraulic conductivity for a 2.54 cm radius well screen. The radius of the well skin is given as the hole radius (R_h).

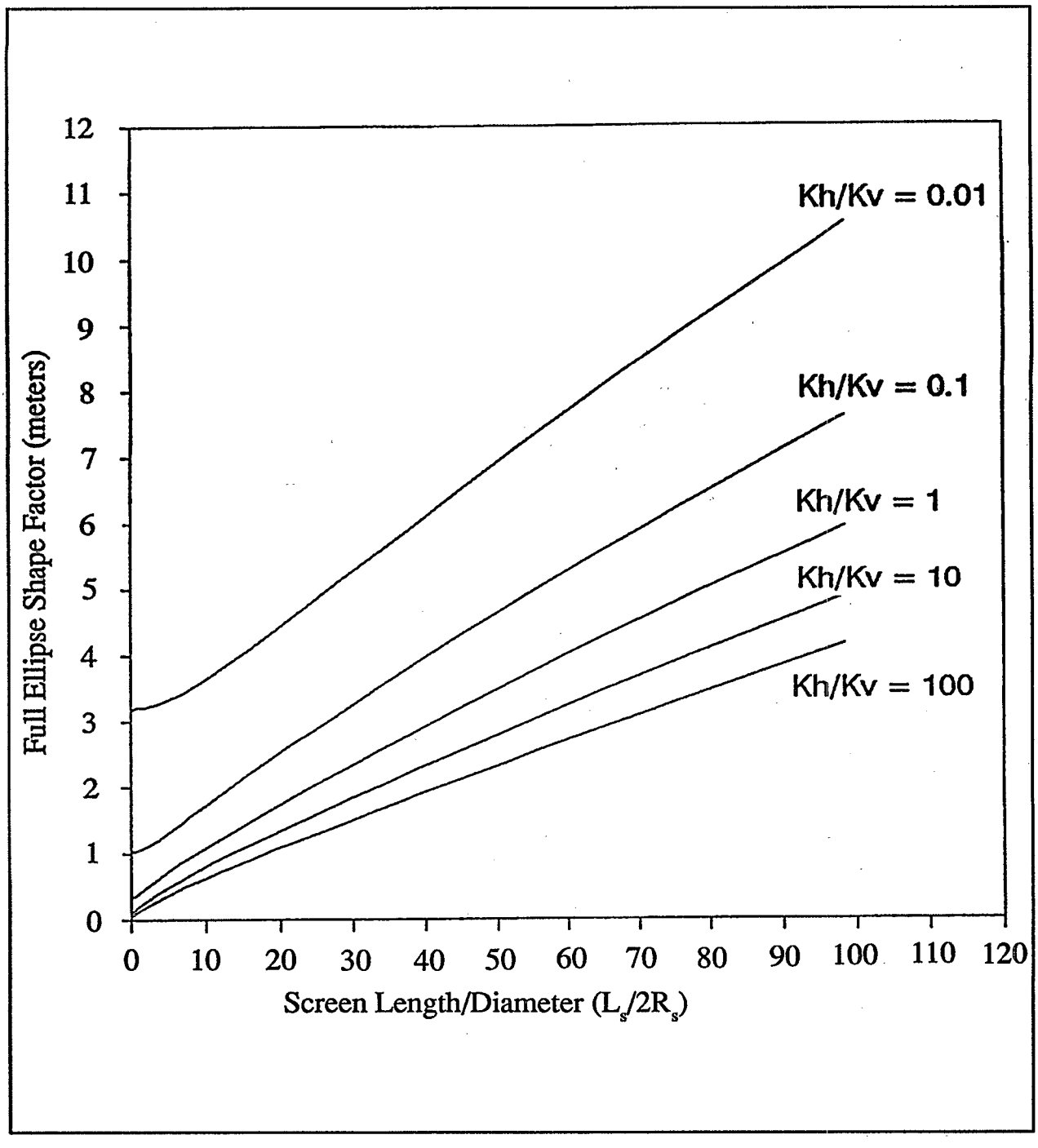

Figure 22. Influence of anisotropy on the full ellipse shape factor for a 2.54 cm radius well screen. K_h and K_v correspond to the horizontal and vertical hydraulic conductivities, respectively.

in the direction of fluid flow. Slug tests in formations with layered heterogeneities will therefore reflect a weighted average of the hydraulic conductivities of the layers intercepted by the screen section of the well. Several authors have evaluated and/or incorporated the effects of anisotropy on slug tests (Maasland, 1955; Widdowson et al., 1990; McElwee et al., 1990; Hvorslev, 1951; and Braester and Thunvik, 1984). Unfortunately, anisotropy ratios are scale dependent and difficult to measure. Small scale anisotropy ratios may be determined with oriented, undisturbed core samples, while large scale anisotropy ratios may be estimated with slug tests conducted in multi-level piezometers or from boring logs.

The effects of anisotropy in soil was first considered by Samsioe (1931) and Dachler (1936), and has been summarized in Hvorslev (1951). The influence of different horizontal (K_h) and vertical (K_v) hydraulic conductivities in two dimensions may be accounted for by dividing the horizontal dimensions of the half and full ellipse shape factors by an anisotropy correction factor m_a:

$$m_a = \sqrt{K_h/K_v} \tag{50}$$

For the half and full ellipse models with $L_s/2R_c > 4$, the horizontal hydraulic conductivity, K_h may be expressed as Equations 51 and 52, respectively.

$$K_h = \frac{(R_c^2)\ln(2m_aL_s/R_c)}{2L_s}\ \frac{\ln(H_1/H_2)}{t_2-t_1} \tag{51}$$

$$K_h = \frac{(R_c^2)\ln(m_aL_s/R_c)}{2L_s}\ \frac{\ln(H_1/H_2)}{t_2-t_1} \tag{52}$$

The effects of anisotropy on the calculated hydraulic conductivity was investigated by comparing the shape factor for the full ellipse model for isotropic conditions (Equations 9) with the shape factor for the full ellipse model for anisotropic conditions (Equations 52). The comparison of the two full ellipse shape factors is shown in Figure 22 for anisotropy ratios (K_h/K_v) equal to 0.01, 0.1, 1.0, 10, and 100. The well used for the calculation was naturally developed with a 2.54 cm radius screen ranging from 0.15 to 4.57 meters in length. An anisotropy ratio greater than 1 resulted in reducing the shape factor. An anisotropy ratio less than 1 resulted in increasing the shape factor. Recall that an increase in the shape factor results in a proportional decrease in the hydraulic conductivity and vice-versa. For cases where the horizontal conductivity is greater than the vertical, anisotropy will increase the calculated horizontal conductivity relative to the isotropic case. As such, ignoring this anisotropy would have resulted in underestimating the hydraulic conductivity in the horizontal direction. The opposite effect would be the case for anisotropy ratios less than 1. It should be re-emphasized that in most cases, the aquifer is assumed to be isotropic in analyzing slug tests, resulting in underestimating the horizontal hydraulic conductivity.

Braester and Thunvik (1984) evaluated the effects of different anisotropy ratios on flow to a partially penetrating well. Steady state flow to a well was calculated using numerical methods for different anisotropic conditions using well and aquifer parameters described in Chapter 3.3. They then compared the hydraulic conductivity obtained using the isotropic solution of Dagan (1978) to the value of the actual horizontal hydraulic conductivity. This comparison is shown graphically in Figure 23. For the case when K_h/K_v was equal to 0.1 and 0.01, they found that Dagan's solution overestimated the horizontal conductivity by a factor of 1.8 and 3.9, respectively. For the case when K_h/K_v was equal to 10 and 100, Dagan's solution underestimated the actual horizontal conductivity by a factor of 0.94 and 0.7.

In addition to anisotropy of hydraulic conductivity, layered heterogeneities are also common due to natural deposition. If a well intercepts more than one layer, the determined horizontal conductivity will be an average of the intercepted layers, weighted to the thickness and conductivity of each of the layers. Assuming horizontal layering, radial flow and an equal head drop radially from the well in each of the layers, the effective hydraulic conductivity (K_{eff}) may be expressed as a simple weighted sum of i layers of thicknesses d_i and conductivities K_i, with a total thickness d_T as shown below (Freeze and Cherry, 1979):

$$K_{eff} = \sum \frac{d_i}{d_T} K_i \qquad (53)$$

PARTIAL PENETRATION AND BOUNDARY EFFECTS

Partially penetrating wells occur when a well screen does not penetrate the full thickness of an aquifer. In this case, flow may no longer be strictly radial and the vertical component of flow may be significant. If vertical flow is important, the radial flow models (e.g., the doughnut model) will overestimate the hydraulic conductivity. If, however, the vertical component is not significant, as may be the case in anisotropic conditions or where the screen length is long, flow to the partially penetrating well may be considered radial and fully penetrating slug test solutions may be used. The influence of partial penetration on slug test results will be a function of the proximity of the screen to the lower impermeable boundary and the degree of anisotropy.

The effects of partial penetration and boundary conditions have been incorporated into the shape factors of the 1/2 ellipse, full ellipse, and doughnut models, as well as into the curve matching solutions. The effect of a lower or upper impermeable boundary on the shape factor S_f for a cylindrical cavity (simulated screen section) was evaluated by a 3-D electric analog by Luthin and Kirkham (1949) and Youngs (1968). Luthin and Kirkham found that the shape factor increased as the cavity approached the water table, and decreased when the cavity approached the lower confining unit. Youngs (1968), using the same 3-D electric analog employed by Smiles and Youngs (1965), evaluated the influence of a lower impermeable substratum for a wider range of well geometries. Youngs found that the shape

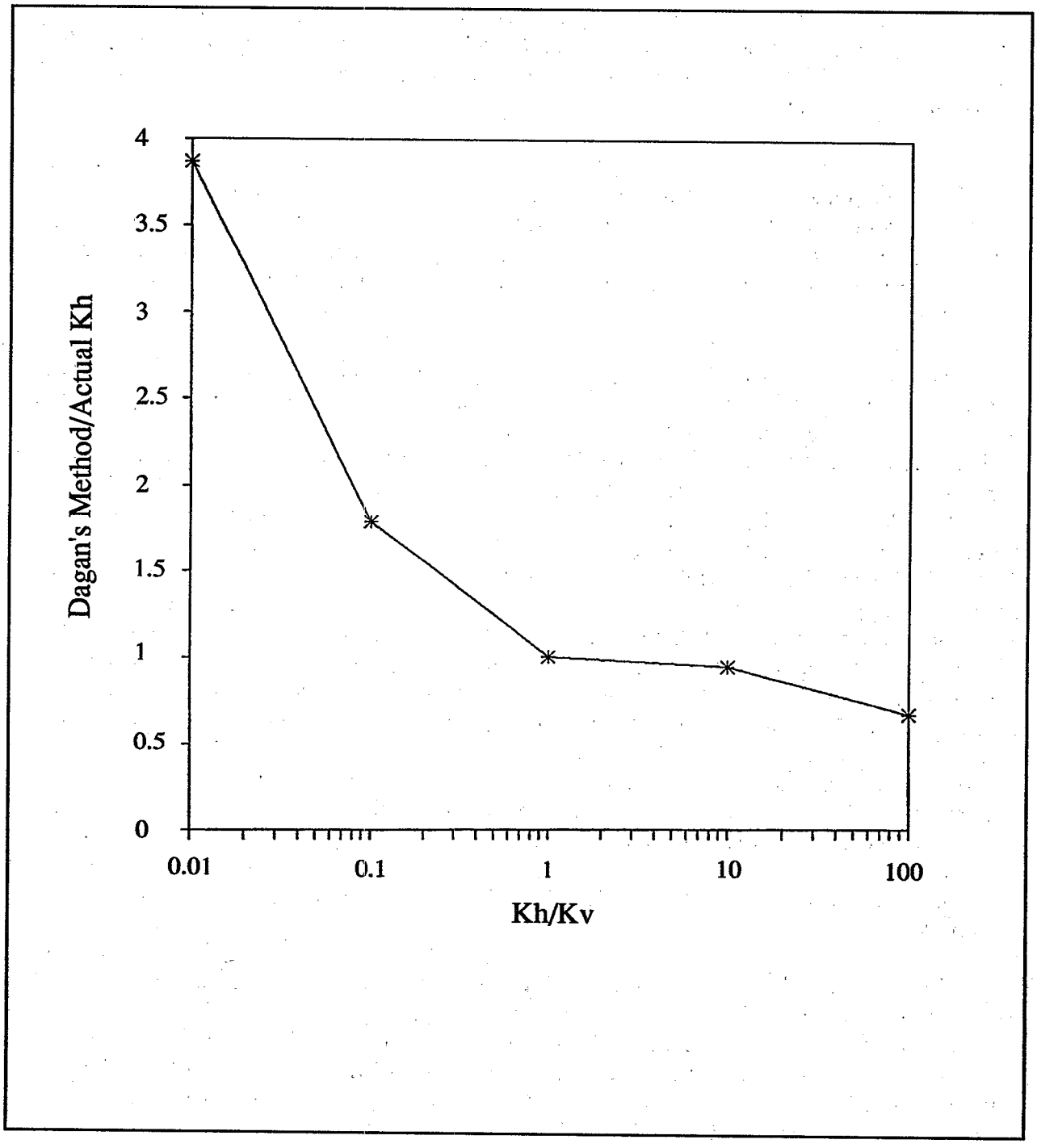

Figure 23. Comparison of the isotropic hydraulic conductivity of Dagan (1978) with the anisotropic conductivity of Braester and Thunvik (1984); developed using data from Braester and Thunvik.

factors, taking a impermeable boundary into consideration, do not vary by more than 20%, provided the distance between the cavity and the substratum is more than the diameter of the piezometer. As with Luthin and Kirkham, the shape factor decreased as the impermeable substratum approached the cavity.

Dagan (1978) found that if the distance from the water table to the lower impermeable boundary was greater than 1.2 times the distance from the water table to the bottom of the screened section, the effect of the lower boundary was negligible. Widdowson et al. (1990) found that the position of the screened section relative to the impermeable boundary had little effect. The effect was even less pronounced when the horizontal conductivity was greater than the vertical.

Bouwer and Rice (1976) investigated the effects of partial penetration and boundaries on the doughnut model for different well and aquifer geometries. A description of Bouwer and Rice's method is presented in Chapter 2.1. In addition, the method for calculating the $\ln(R_e/R_s)$ term is presented as Equations 29 and 30 for partially and fully penetrating well screens, respectively. An assessment of the Bouwer and Rice method was conducted by first calculating the term $\ln(R_e/R_s)$ and the radius of influence for a fully penetrating 11.43 cm radius, 1.52 meter long screen using Equation 30. The $\ln(R_e/R_s)$ term equaled 1.86 (dimensionless) with a corresponding radius of influence of 0.74 meters. The distance to the lower boundary was then increased from 0 to 20 meters for the same well geometry with the top of the screen at the upper impermeable boundary (i.e., $L_w = L_s$, referring to Figure 12). The $\ln(R_e/R_s)$ term and the radius of influence was calculated using Equation 29. As shown on Figure 24, increasing the distance to the lower boundary had the effect of marginally reducing the $\ln(R_e/R_s)$ term from 1.86 to 1.51 in an exponential manner. The radius of influence also decreased from 0.74 to 0.51 meters. Noting that the hydraulic conductivity of the doughnut model is directly proportional to the $\ln(R_e/R_s)$ term, compensating for partial penetration in the method of Bouwer and Rice would therefore appear to have a negligible effect on the calculated hydraulic conductivity.

FILTER PACK DRAINAGE AND RESATURATION IN PARTIALLY SUBMERGED WELL SCREENS

Removal of a slug of water from a typical monitoring well with a partially submerged screen and filter pack will cause drainage of the filter pack into the well. The degree to which drainage of the filter sand may dominate water level recovery is a function of the contrast between the hydraulic conductivities of the filter sand and the formation. If the filter sand is less permeable than the formation, the determined hydraulic conductivity will be predominantly that of the filter sand (see Chapter 3.3). A well with a filter pack with exactly the same hydraulic properties as the formation may be considered as a naturally developed well. Filter sands are typically coarser than the formation and have a higher hydraulic conductivity, although clogging of the filter pack with fines or biofilm development may reduce the conductivity of the filter sand. If the filter sand is more conductive than the formation, drainage of the filter sand will dominate the recovery rate to the well until the

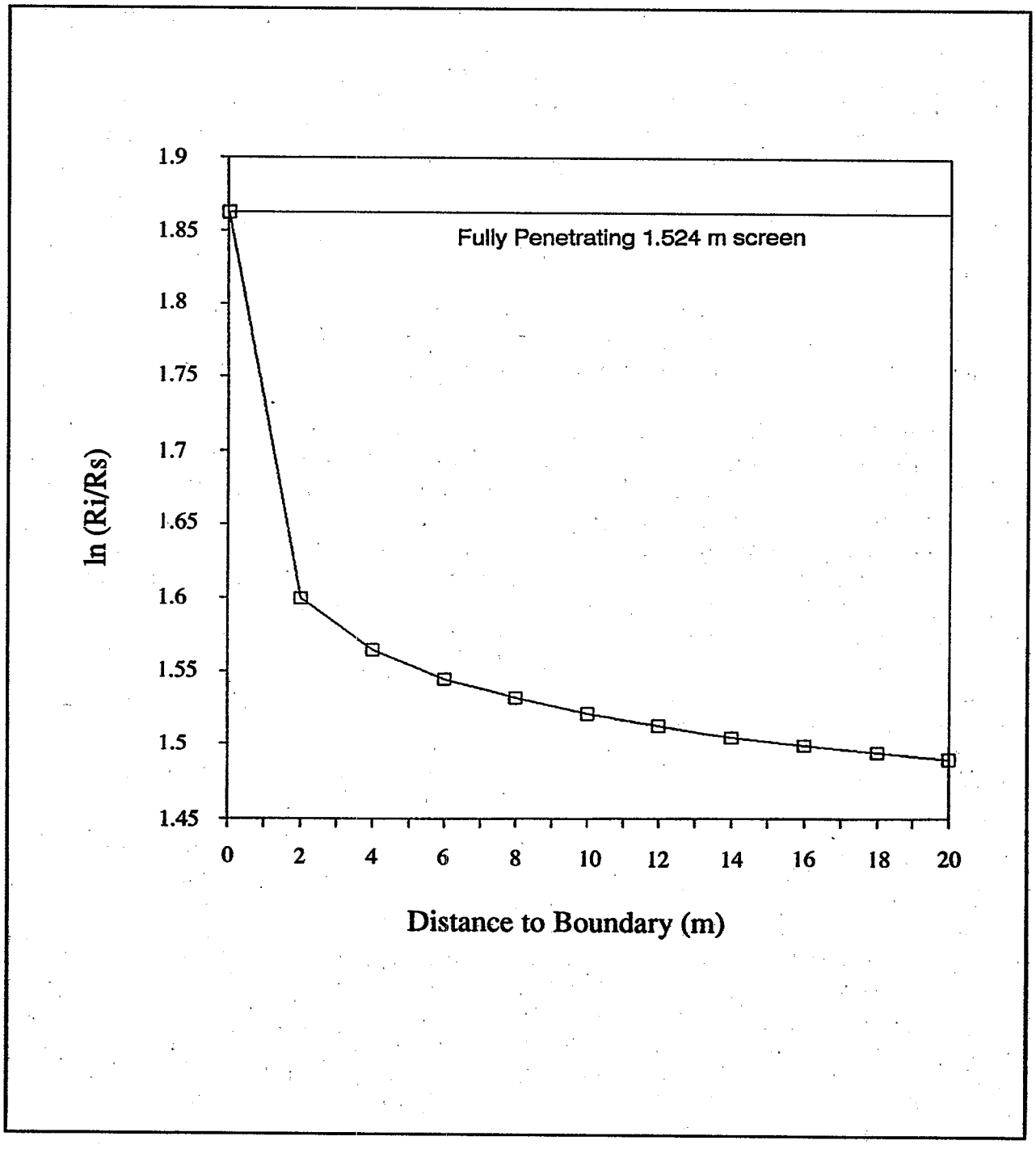

Figure 24. Effects of partial penetration on the $\ln(R_i/R_s)$ term as a function of the distance to a lower impermeable boundary (D') for a 11.43 cm radius, 1.524 meter long, well screen. Using method of Bouwer and Rice, 1976.

filter sand reaches its specific retention. This leaves a desaturated filter sand column of length H_l. A typical recovery curve from a well with a partially submerged screen is shown as Figure 25. As exemplified in the Figure, slug test data from partially submerged wells with highly conductive filter sands typically exhibit a very steep curve in early time representing the filter pack drainage, followed by a log-linear curve in mid-time representing recovery of the casing and the filter sand by the formation, followed by a tailing off of head with time. It is the mid-time, log-linear portion of the recovery curve that should be used for determining the hydraulic conductivity (often very early time data is mistakenly used). The transition between early and mid-time portions of the recovery curve (i.e., the point at which the filter sand effectively stops draining and formation recharge becomes dominant) is a function of the contrast in conductivities between the filter sand and the formation. If the contrast is great, the recovery curve will exhibit a sharp transition. If the contrast in conductivities is not great, then the transition zone may be temporally broad.

Drainage of the filter sand has the effect of significantly reducing the head difference left for recharge by the formation. Ideally the initial head drop caused by removal of a slug of water may be calculated by dividing the volume of a slug removed from the well by the area of the well casing. If the filter pack does not drain, then the calculated initial head drop (H_{oc}) should compare well with the first water level readings collected after removal of the slug. In the case of rapid filter pack drainage, the initial water level readings are typically only a fraction of the calculated initial head drop. The reduction in the initial head drop due to filter pack drainage is a function of the volume and specific yield of the draining sand pack relative to the size of the well casing. The head remaining in the well after filter drainage may be reduced to less than a few tens of centimeters, which implies limited hydraulic stress induced in the formation. A small hydraulic stress in the formation is pertinent to the radius of influence of the test, and consequently. The volume of aquifer tested. A very small radius of influence may also increase the effects of a well skin as was discussed in Chapter 3.3.

The recharge rate to a well is typically measured as the changing water level in a well casing of a given radius. This method is appropriate for fully submerged screened wells with or without a filter pack as long as the filter pack remains saturated at all times. For the case of partially submerged well screens with filter pack drainage, recharge to the well is not only filling the casing, but also an unknown portion of the drained filter pack. The recharge rate of the well, and the resulting hydraulic conductivity, will be underestimated if the desaturated volume of the filter pack is not considered. The additional volume of the filter pack may be accounted for by replacing the casing radius in model solutions by an effective casing radius (R_{cc}). The effective casing radius includes an additional radial increment of account for the resaturation of the filter pack. Slug test solutions are sensitive to error in the casing radius, since the hydraulic conductivity is proportional to the square of this radius.

Bouwer and Rice (1976) and Bouwer (1989) have addressed the drainage and subsequent resaturation of the filter pack. Bouwer suggests increasing the radius of the

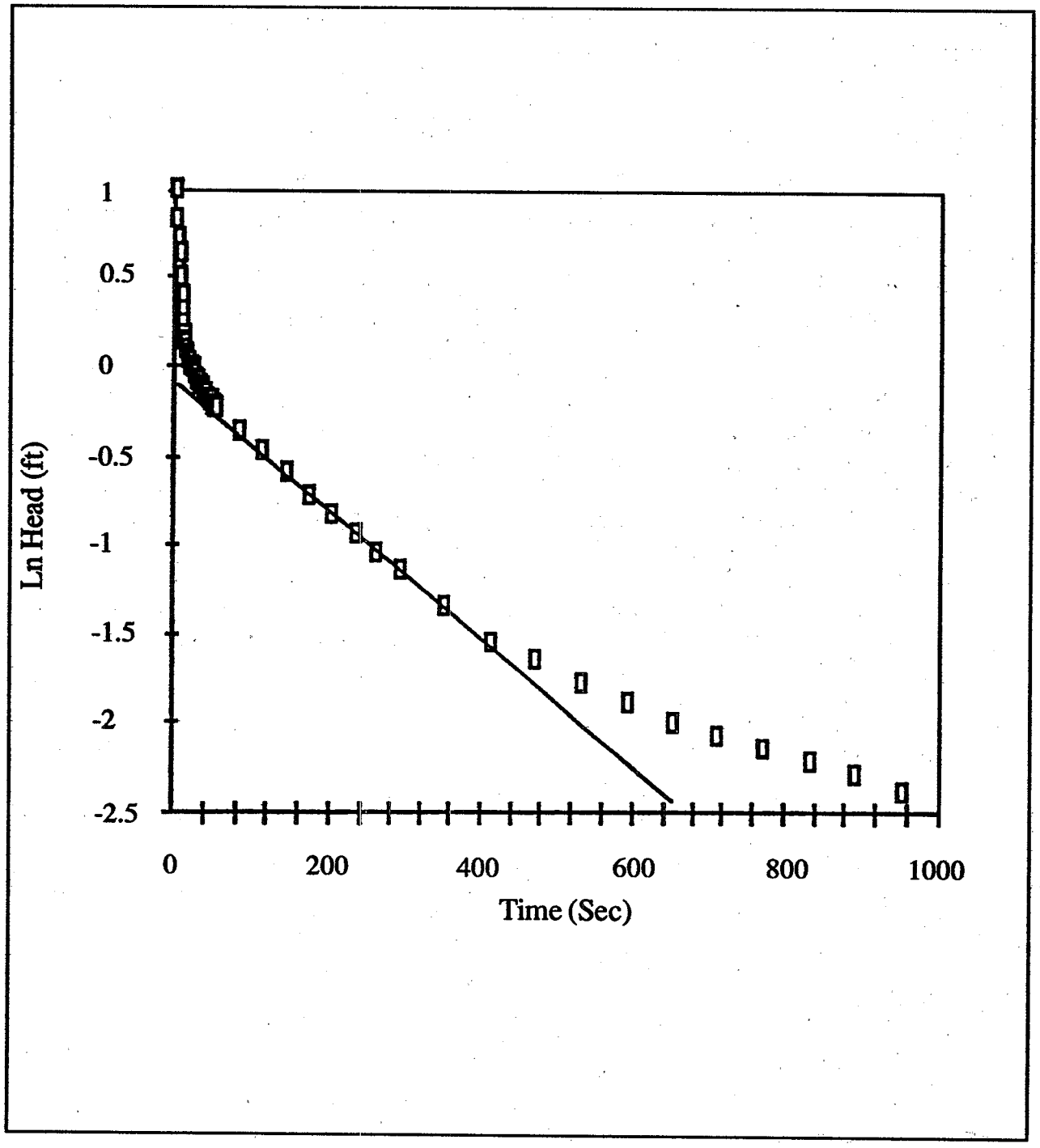

Figure 25. Slug test recovery curve from a typical monitoring well with a partially submerged well screen. Well MMW-8; UCONN Motorpool, August 6, 1991. After Binkhorst, 1992.

casing (R_c) by a fraction equal to the radius of hole (R_h) minus the radius of the casing, multiplied by the porosity (n) of the sand pack:

$$R_{ce} = \sqrt{(1\text{-}n)\ R_c^2 + nR_h^2} \qquad (54)$$

This method provides an estimate of the effective casing radius. The hole dimensions and the porosity of the filter sand must be accurately known. It should be realized that the volume of water that drains from a filter sand is not a function of its porosity, but of its specific yield. Specific yield values for fine to coarse sands typically used for filters may range from 1 to 30% (Freeze and Cherry, 1979), while the porosity may range from 15 to 48% (de Marsily, 1986). Using the porosity for the determination of the effective casing radius may overestimate the volume of sand to be recharged and the hydraulic conductivity. If the borehole is larger than the auger flights, due to formation caving or drill stem wobble, the effective casing radius would be underestimated and consequently, the hydraulic conductivity would be overestimated. The range of error involved in accounting for resaturation of the filter sand was assessed for a typical monitoring well geometry. The well geometry consisting of a 5.08 cm diameter well in a 22.86 cm diameter hole with a coarse filter sand having a 45% porosity. The range of error using this geometry was calculated as approximately one order of magnitude. For the same geometry, a range of error was calculated using the filter sand porosity (45%) versus a hypothetical specific yield of 10%. Using the porosity, the resultant hydraulic conductivity would have been overestimated by approximately one third an order of magnitude or 330%.

As part of this study, a method has been developed to determine an effective specific yield of the filter pack surrounding the well, and to calculate an effective casing radius. This method assumes that hysteresis effects between wetting and drying is negligible and that the volume of water released from the filter sand is small at late time relative to flow from the formation. The method uses the early recovery data from typical monitoring wells to calculate the volume of water released from the filter sand, as well as the volume of filter sand from which it was released. Parameters are illustrated in Figure 26.

An initial drawdown, H_{oc}, in a well without filter pack drainage can be calculated by equating the volume of water removed from the well (V_b) to an equal volume in the well casing (V_c), Equation 55. The volume of the well casing is equivalent to the H_{oc} multiplied by the area of the well casing (A_w), using the inside radius of the casing (R_{ci}) as in Equation 56. The volume of the bailer (V_b), may be calculated from Equation 57 using the outside radius (B_{or}) and length (B_l) of the bailer. Equating 56 and 57 and solving in terms H_{oc} yields Equation 59 to calculate the initial drawdown.

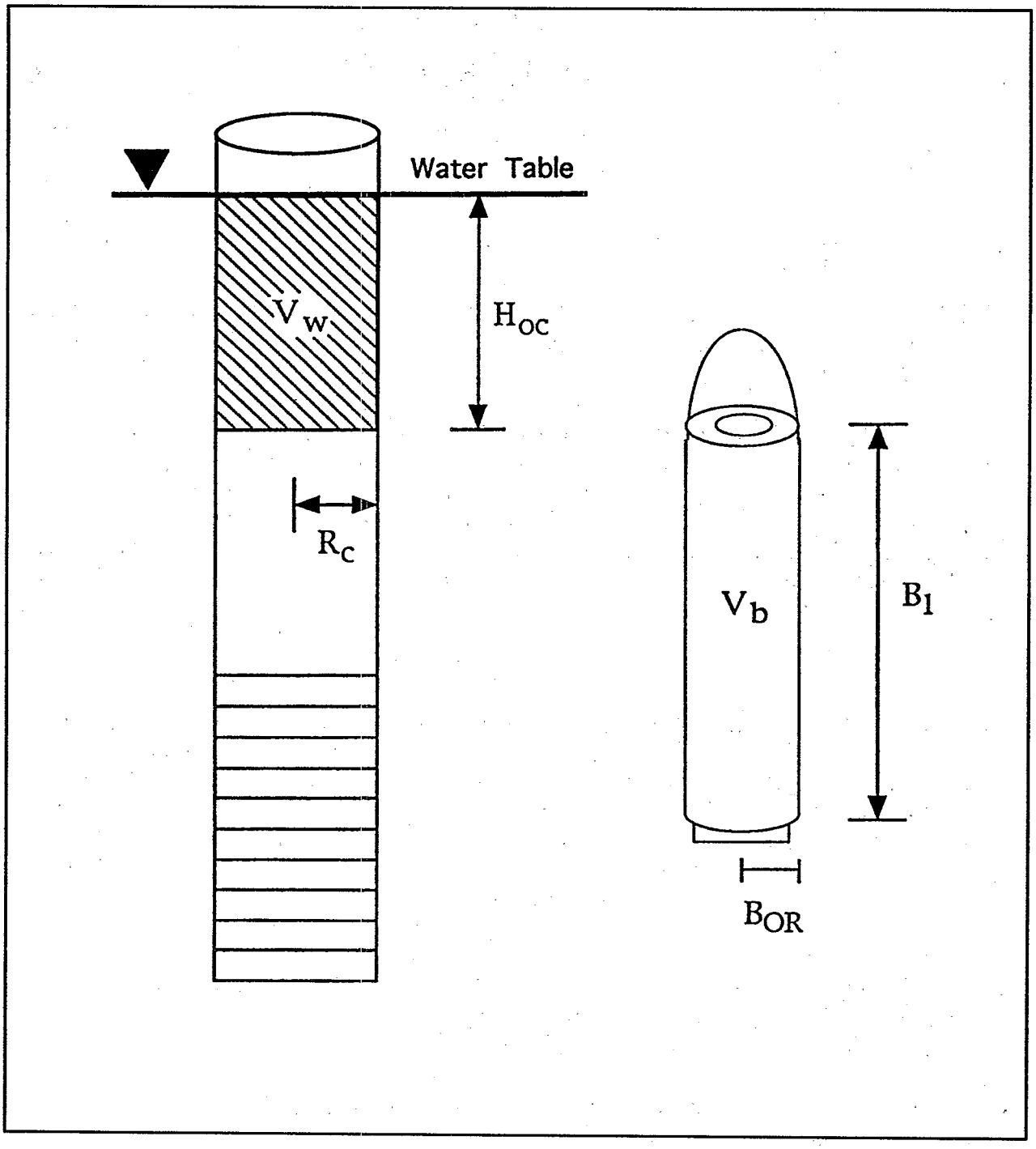

Figure 26. Illustration of parameters needed to calculate the initial head drop.

$$V_b = V_c \tag{55}$$

$$V_c = H_{oc}A_w = H_{oc}\pi R_{ci}^2 \tag{56}$$

$$V_b = \pi B_{or}^2 * B_l \tag{57}$$

$$H_{oc} = \frac{V_b}{A_w} \tag{58}$$

The bailer must be fully submerged, and the aquifer re-equilibrated prior to bailer removal or the calculated initial drawdown will be overestimated. The specific yield of a sand is equal to the volume of water that may be drained per volume of sand.

The effective specific yield of the sand pack can be determined by using the initial drawdown (H_{oc}), as calculated from the bailer dimensions, and the head at which the sand effectively stops draining. This head may be determined graphically from the natural log of head versus time plot as the head (H_l) at which log-linear recovery of the well commences. This method is illustrated in Figure 27. The volume of water released from the sand (V_w) may be calculated from the difference between H_{oc} and H_1, multiplied by the inside area of the well casing:

$$V_w = \pi R_{ci}^2 * (H_{oc} - H_l) \tag{59}$$

As shown in Figure 28, the volume of sand from which the water drained must be situated above H_l. In cases of highly conductive formations, a fraction of water may also come from the formation during filter sand drainage, resulting in a broad transition zone and potential over-estimation of the volume of water that actually drained from the sand pack. The volume of sand (V_s) in the filter pack above the head at which linear recovery commenced may be calculated from the radius of the hole (R_h), the outside radius of the screen (R_{co}), and H_l:

$$V_s = \pi(R_h^2 - R_{co}^2) * H_l \tag{60}$$

An effective specific yield of the sand (S_y) may then be calculated using Equation 61. This method assumes that the specific yield of the filter pack is uniform. Error in the hole dimensions will be transferred to error in the specific yield. If the hole diameter and, thus, the actual volume of sand is underestimated, the specific yield of the sand as calculated from Equation 61 will be overestimated. This error is self-correcting when the effective casing radius is calculated (see below).

$$S_y = \frac{V_w}{V_s} 100\% \tag{61}$$

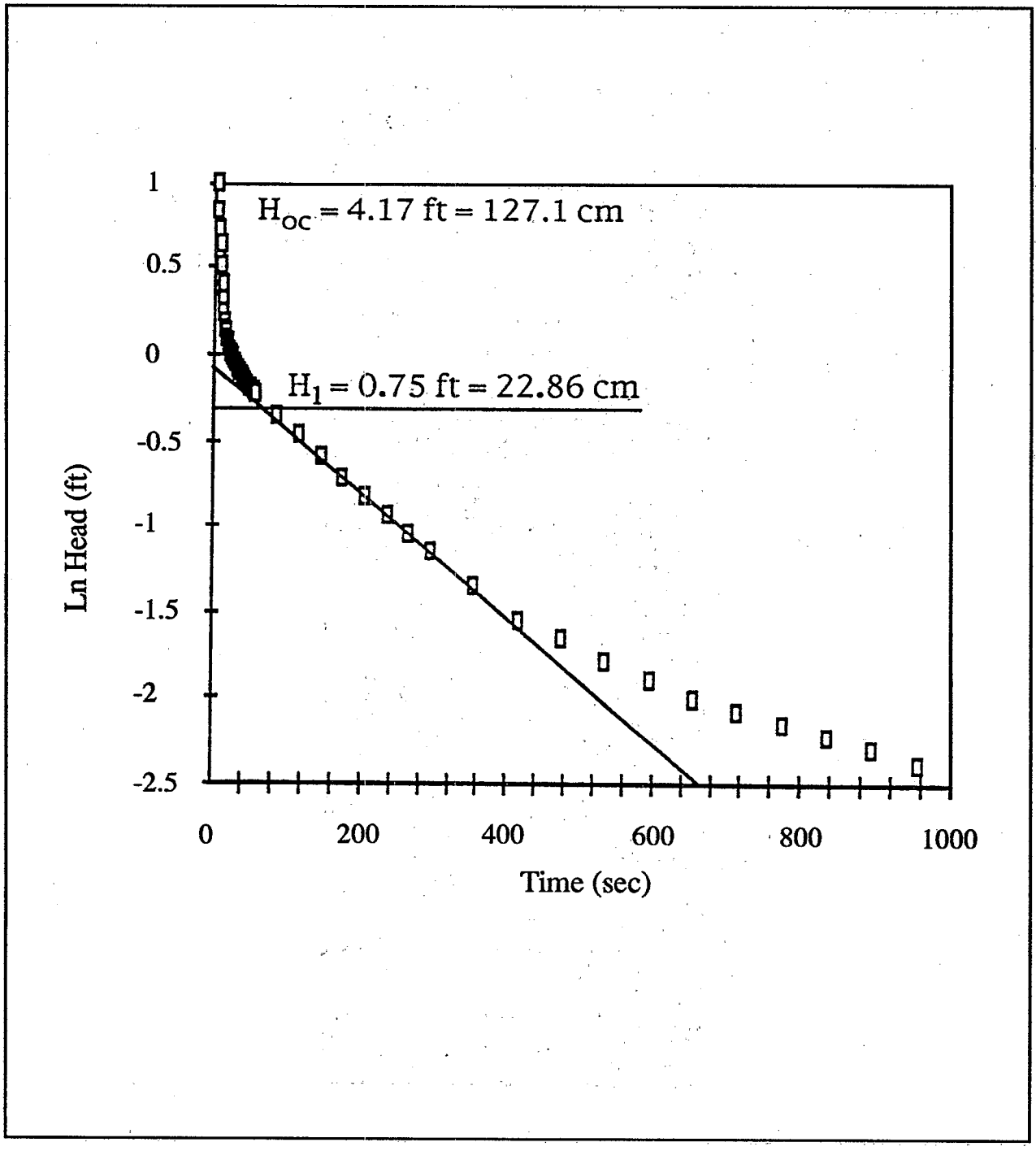

Figure 27. Determination of the transition point (H_1) on the recovery curve of a typical monitoring well with a partially submerged screen exhibiting filter sand pack drainage in early time.

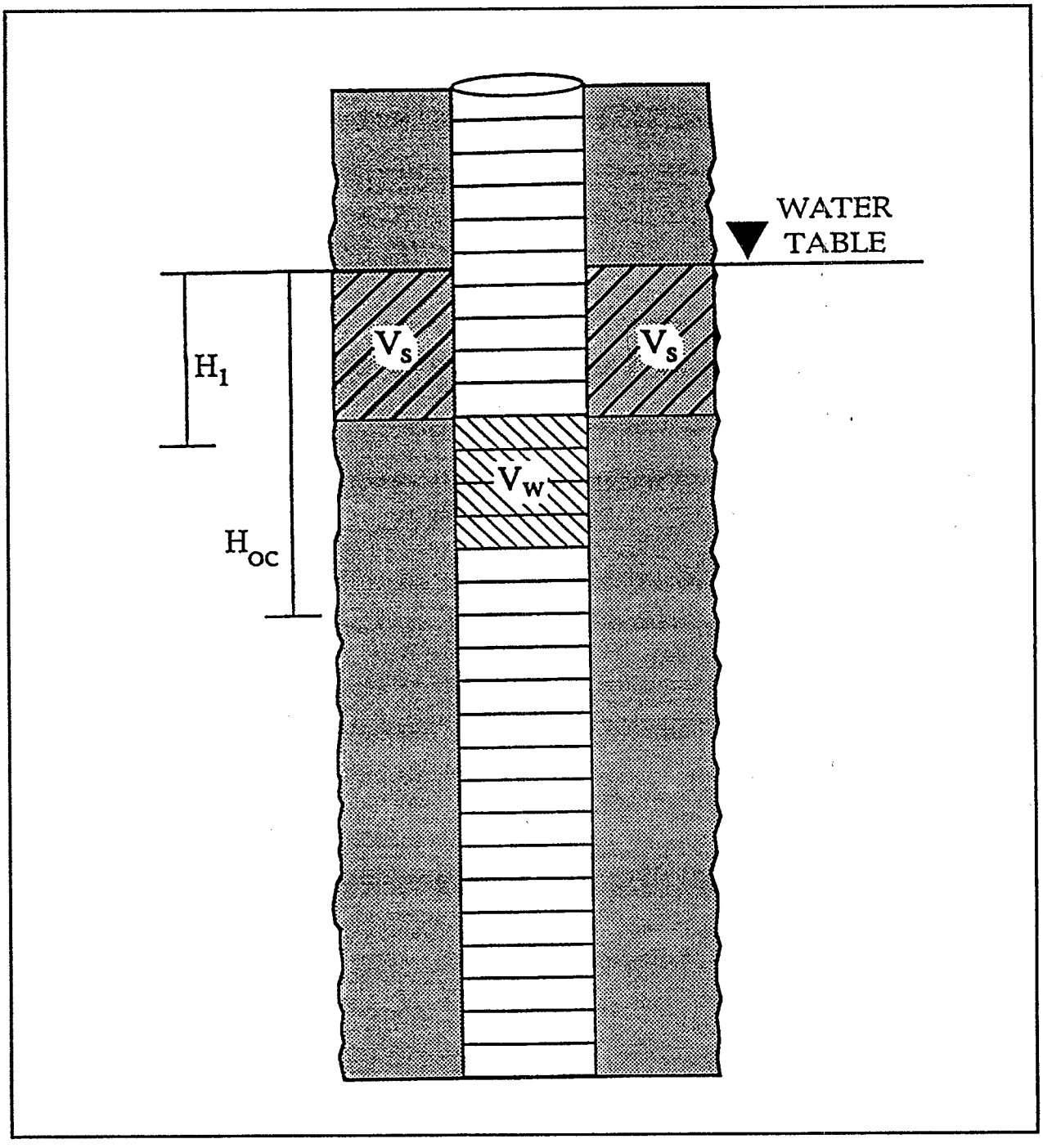

Figure 28. Illustration of parameters used to estimate the specific yield of the filter sand pack from early time recovery data.

Take for an example, a 5.21 cm I.D./5.97 cm O.D. well screen surrounded by a filter pack installed in a 22.86 cm hole. A slug test in this well using a 0.91 meter, 4.13 cm O.D. bailer resulted in rapid sand pack drainage early in the test. Linear recovery was observed to commence at 0.12 meters of head in the well. The total volume of the bailer (V_b) was calculated using Equation 57 as 1.22×10^{-3} m^3. The area of the inside of the well casing (A_w) was calculated (Equation 56) to be 6.49×10^{-4} m^3. Using these values and Equation 58, the calculated initial drawdown in the well (H_{oc}) was estimated to be 0.575 meters. The volume of water released from the sand using Equation 59 is 9.63×10^{-4} m^3. The volume of sand where the water was released is 4.75×10^{-3} m^3 using Equation 60. From Equation 61, the specific yield is calculated to be 20.3%.

Once the effective specific yield of the sand pack has been determined, an effective casing radius (R_{ce}) can be calculated using Equation 54, by substituting the specific yield for the porosity term, and by using the inside and outside radii of the well casing:

$$R_{ce} = \sqrt{R_{ci}^2 + S_y (R_h^2 - R_{co}^2)} \qquad (62)$$

For the above example, the effective casing radius would be calculated as 5.7 cm using Equation 62. Calculation of the effective casing radius is independent of potential error in the specific yield resulting from poor control on the actual hole dimensions. This error will be canceled out in Equation 62, since both the specific yield and the hole radius terms include the inaccurate hole dimensions.

REDUCTION OF SCREEN INTAKE LENGTH IN PARTIALLY SUBMERGED SCREEN WELLS

The screen intake length of a fully submerged screen well remains constant during a slug test. However, removal of a slug of water from a well with a partially submerged screen causes denaturation of the screen and filter sand. The formation can contribute to the recovery of the well only through the saturated portion of the well screen. Hence, denaturation of the filter sand effectively reduces the screen length. The effective screen length would be at a minimum at the beginning of the test and increase as the screen and filter sand are resaturated.

The importance of this effect would be a function of the desaturated screen length relative to the overall screen length. In typical 5.08 cm diameter monitoring wells in 22.86 cm diameter holes, the desaturated screen length after filter sand drainage can typically be less than 15 cm, while the overall screen length may range from 1 to 5 meters. To assess the importance of screen denaturation, Figure 29 was generated. The Figure shows how shape factor for the full ellipse model would decrease with increasing screen denaturation for wells having initial screen lengths equal to 1, 2, and 5 meters. Recall that the hydraulic conductivity is inversely proportional to the shape factor. Therefore, if screen denaturation is

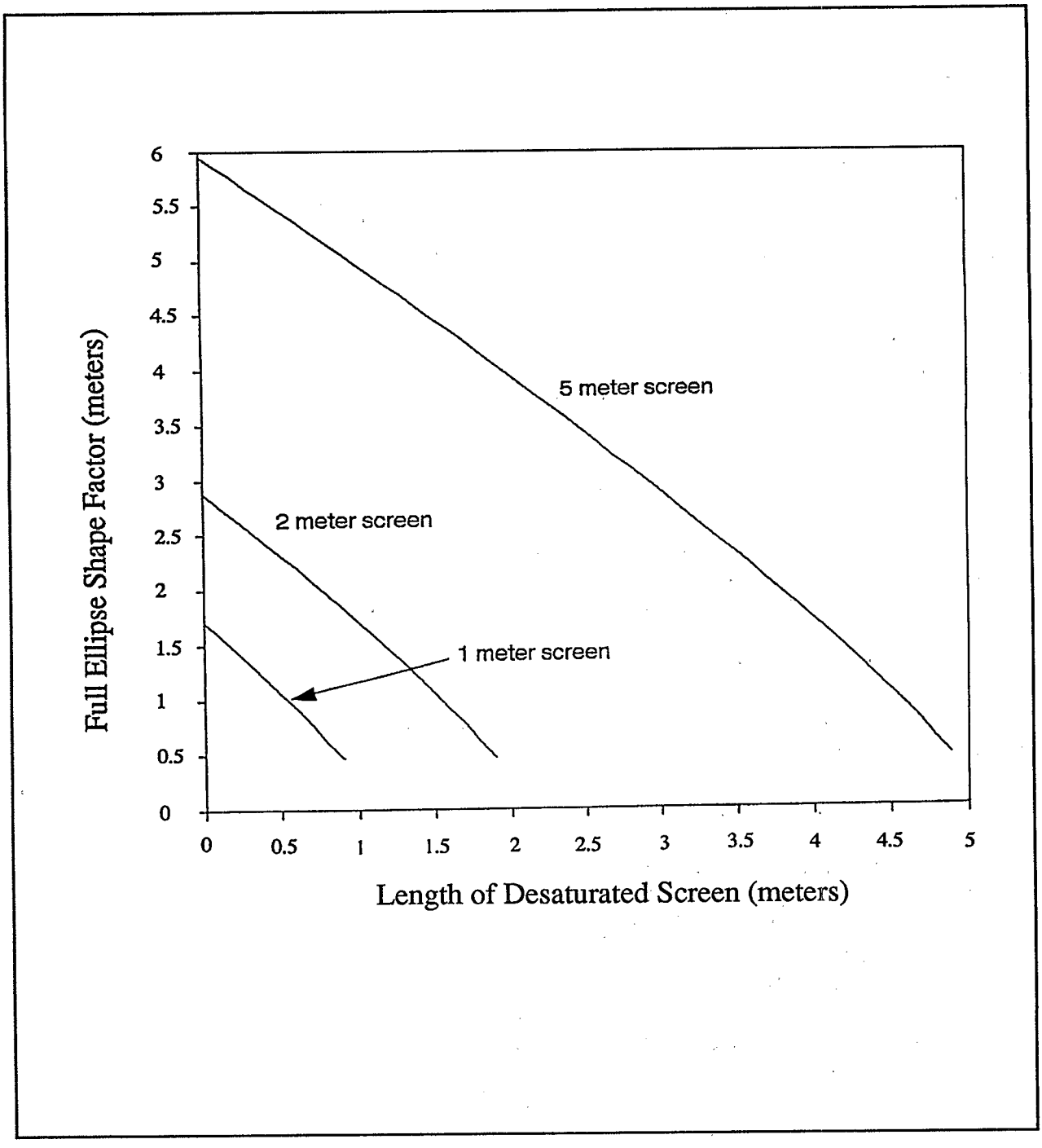

Figure 29. Changes in the full ellipse model shape factor caused by screen length reduction resulting from filter sand pack drainage for a 11.43 cm radius borehole.

not accounted for, the hydraulic conductivity will be underestimated. Since the effective screen length will vary during water level recovery, the log-linearity of the recovery curves can be affected. This further complicates determining a meaningful hydraulic conductivity value for wells with partially submerged screens.

SECTION 4

SUMMARY, CONCLUSIONS AND RECOMMENDATIONS

Slug tests provide a useful means of estimating a formation's hydraulic conductivity in the near vicinity of the screened interval of the well. Slug tests have the advantage of being relatively rapid, inexpensive, and involve removal of little or no potentially contaminated water. However, it has been shown that the evaluated hydraulic conductivity may be affected by many factors, including the approximation of shape factors, evaluation of the radius of influence, well skin effects, formation anisotropy and heterogeneities, and development of a cone of depression. Also, in typical monitoring wells with partially submerged screen sections calculation of hydraulic conductivity may be affected by drainage of the filter sand, resaturation of an unknown percentage of the filter pack, a dramatic reduction in the initial head drop due to filter sand pack drainage, and a non-constant screen intake length over the course of the test. The effect of these factors on the evaluated hydraulic conductivity is a function of the well geometry and construction, formation properties and the mathematical models used for interpretation of the slug test data.

Sensitivity analyses yielded the following conclusions:

1) Available full ellipse shape factors vary by less than a factor of 2. The full ellipse shape factor summarized by Hvorslev (1951) provides a workable average for a typical monitoring well geometry.

2) The doughnut shape factor is exact for the model geometry, but contains an unknown radius of influence. The doughnut shape factor is sensitive to changes in the radius of influence, if the radius of influence is small, e.g., less than approximately 2 meters. A mass balance approach to the volume of water removed indicates that the radius of influence for a typical monitoring well may be less than this value.

3) The Bouwer and Rice method is the only available method to calculate the radius of influence for the doughnut model. However, the method does not account for formation properties and the magnitude of the initial head exchange. Using the Bouwer and Rice method, the radius of influence was found to be equal to approximately one third of the screen length for the typical monitoring well geometry.

4) Slug tests are very sensitive to a less permeable well skin, resulting in significant underestimation of the formation's hydraulic conductivity. Given this sensitivity, wells must be carefully constructed and drilled to minimize formation disturbance and entrapment of fines. In addition, well should be well developed.

5) Overestimation of the formation conductivity due to a more permeable well skin may be overcome by increasing the radius of influence with a greater initial head change.

6) Slug tests provide a weighted average conductivity of formations that intersect the well screen provided that the screen section remains fully submerged. This effect may be minimized by constructing wells screened in discrete formations.

7) Slug tests do not appear sensitive to formation anisotropy, if the horizontal conductivity is greater than the vertical.

8) For wells with filter sand packs, the radius of the borehole should be used as the intake radius in slug test solutions.

With specific reference to a well with a partially submerged screen section:

9) The problems associated with this well geometry are best overcome by only using fully submerged well screens for slug testing.

10) Water level recovery in a typical monitoring well in early time is dominated by rapid draining of the filter sand evidenced by a steep portion of the recovery curve in early time. Hence, this portion of the recovery curve should not be used in calculating hydraulic conductivity. Calculation of hydraulic conductivity using the early portion of the recovery curve may overestimate the formation conductivity by over an order of magnitude.

11) Tailing off of recovery data in late time is a result of the development of a cone of depression. Using the late time data may underestimate the formation conductivity.

12) The middle log-linear portion of recovery data from typical monitoring wells represents recharge of the well and the filter sand by the formation. Interpretation of this portion of the recovery curve must include resaturation of the sand pack's specific yield, or the calculated hydraulic conductivity will be underestimated. Use of the filter sand porosity as opposed to the specific yield may result in significant overestimation of the formation conductivity.

13) Slug-in or mandrel-in tests should not be conducted in wells with partially submerged screen sections due to saturation of the unsaturated filter sand and formation.

14) A method was presented to calculate the sand pack's specific yield from early recovery data, and to incorporate the specific yield into slug tests solutions with an effective casing radius. This method assumes a uniform specific yield along the length of the desaturated filter sand column. The method may be used when there is a sharp transition in the recovery curve between filter sand drainage and formation recharge.

15) To use Hvorslev's (1951) Time Lag Method for slug tests in typical monitoring wells with a rapid initial recharge, the initial head drop should be regressed as the Y-intercept of the middle log-linear recovery data.

16) The great reduction in initial head drop associated with filter pack drainage may increase well skin effects by reducing the radius of influence. This head reduction may be reduced using filter sands with lower specific yields and by reducing the annular space between the well screen and the hole. This effect may also be reduced by increasing the volume of the slug out.

17) A reduction in screen intake length due to filter pack drainage was determined not to be significant unless the desaturated screen length becomes large relative to the overall screen length.

REFERENCES

Al-Dhahir, Z.A. and N.R. Morgenstern. 1969. Intake factors for cylindrical piezometer tips. Soil Science, v. 107, no. 1, pp.17-21.

Barker, J.A. and J.H. Black. 1983. Slug tests in fissured aquifers. Water Resources Research, v. 19, no. 6, pp. 1558-1564.

Binkhorst, G.K. 1992. Evaluation of Slug Test Methods for Determining Hydraulic Conductivity in Unconfined Aquifers. Unpublished M.S. Thesis. University of Connecticut. 256 pages.

Bouwer, H. and R.C. Rice. 1976. A slug test method for determining hydraulic conductivity of unconfined aquifers with completely or partially penetrating wells. Water Resources Research, v. 12, no. 3, pp. 423-428.

Bouwer, H. 1989. The Bouwer and Rice slug test - an update. Ground Water, v. 27, no. 3, pp. 304-309.

Braester, C., and R. Thunvik. 1984. Determination of formation permeability by double packer tests. Journal of Hydrology, v. 72, pp. 375-389.

Brand, E.W. and J. Premchitt. 1980. Shape factors of cylindrical piezometers. Geotechnique, v. 32, no. 3, pp. 203-216.

Bredehoeft, J.D. and S.S. Papadopulos. 1980. A method for determining the hydraulic properties of tight formations. Water Res. Research, v. 16, no. 1, pp. 233-238.

Bredehoeft, J.D., H. Cooper, Jr., and I.S. Papadopulos. 1966. Inertial and storage effects in well-aquifer systems: An analog-investigation. Water Resources Research, v. 2, no. 4, pp. 697-707.

Butler, J.J. 1990. The role of pumping tests in site characterization: some theoretical considerations. Ground Water, v. 28, no. 3, pp. 394-402.

Carslaw, H.S. and J.C. Jaeger. Conduction of Heat in Solids. 2nd edition, Oxford University Press, New York, 1959.

Chapuis, R.P. 1989. Shape factors for permeability tests in boreholes and piezometers. Ground Water, v. 27, no. 5, pp. 647-654.

Chirlin, G.R. 1989. A critique of the Hvorslev method for slug test analysis: the fully penetrating well. Ground Water Monitoring Review, v. 9, no. 2, pp. 130-138.

Cooper, H.H., J.D. Bredehoeft, and S.S. Papadopulos. 1967. Response of a finite-diameter well to an instantaneous charge of water. Water Resources Research, v. 3, no. 1, pp. 263-269.

Dachler, R. 1936. Grundwasserstromung (Flow of Ground Water). Julius Springer, Wein. 141 p.

Dagan, G. 1978. A note on packer, slug and recovery tests in unconfined aquifers. Water Resources Research, v. 14, no. 5, pp 929-934.

Dax, A. 1987. A note on the analysis of slug tests. Journal of Hydrology, v. 91, pp. 153-177.

Dougherty, D.E. and D.K. Babu. 1984. Flow to a partially penetrating well in a double porosity reservoir. Water Resources Research, v. 20, no. 8, pp. 1116-1122.

Faust, C.R. and J.W. Mercer. 1984. Evaluation of slug tests in wells containing a finite-thickness skin. Water Resources Research, v. 20, no. 4, pp. 504-506.

Ferris J.G and D.B. Knowles. 1954. The slug test for estimating transmissibility. U.S.G.S. Ground Water Note 26, pp. 1-7.

Forchheimer, Ph. 1930. Hydraulik, 3rd edition. B.G. Teubner, Leipzig und Berlin. 596 pp.

Freeze, R.A. and J.A. Cherry. 1979. Groundwater. Englewood Cliffs, New Jersey.

Frevert, R.K. and D. Kirkham. 1948. A field method for measuring the permeability of soil below the water table. Highway Research Board, Proc. 28, pp. 433-442.

Hooghoudt, S.B. 1936. Bepaling van den doorlaatfactor van den grond met behulp van pompproeven, (z.g. boorgatenmethode). Verslag Landbouwk. Onderzoek 42, pp. 449-541.

Hubbert, M.K. 1940. The theory of ground-water motion. Jour. Geology, v. 48, no. 8, pt. 1, pp. 785-944.

Hvorslev, H.J. 1951. Time lag and soil permeability in ground-water observations. Waterways Experiment Station, Corps of Engineers, U.S. Army, Vicksburg, M.S. Bulletin No. 36.

Jacob, C.E. 1940. On the flow of water in an elastic artesian aquifer. Trans. American Geophysical Union, v. 21, pp. 574-586.

Jacob, C.E. 1950. Flow of groundwater, in Engineering Hydraulics, edited by H. Rouse, John Wiley & Sons, New York.

Jaeger, J.C. 1956. Conduction of heat in an infinite region bounded internally by circular cylinder of a perfect conductor. Aust, J. Phys., vol. 9, no. 2, p. 167.

Kallstenius, T. and A. Wallgren. 1956. Pore pressure measurements in field investigations. Proceedings of the Royal Swedish Geotechnical Inst. no. 13

Karasaki, K., J.C.S. Long, and P.A. Witherspoon. 1988. Analytical models of slug tests. Water Resources Research, v. 24, no. 1, pp. 115-126.

Kipp, K.L. 1985. Type curve analysis of inertial effects in the response of a well to a slug test. Water Resources Research, v. 21, nO. 9, pp. 1397-1408.

Kirkham, D. 1946. Proposed method for field measurement of permeability of soil below the water table. Soil Society of America Proceedings, v. 10, pp. 58-68.

Lohman, S.W. 1972. Ground-Water Hydraulics. U.S. Geological Survey. Professional Paper 708.

Luthin, J.N. and D. Kirkham. 1949. A piezometer method for measuring permeability of soil in-situ below a water table. Soil Science, v. 68, pp. 349-358.

Maasland, M. 1955. Measurement of hydraulic conductivity by the auger hole method in anisotropic soil. Soil Science. v. 81, pp. 379-388

de Marsily, G. 1986. Quantitative Hydrogeology. Academic Press, Inc. San Diego, CA.

McElwee, C.D., J.J. Butler Jr., W. Liu and G.C. Bohling. 1990. Effects of partial penetration, anisotropy, boundaries and well skin on slug tests. Kansas Geological Survey Report No. 90-13. Prepared for presentation at The American Geophysical Union Spring Meeting in Baltimore, Maryland; May 30, 1990.

Meinzer, O.E. 1923. Outline of ground-water hydrology, with definitions. U.S. Geological Survey Water-Supply Paper 494-C, 71 p.

Moench, A.F. and P.A. Hsieh. 1985. Comment on "Evaluation of slug tests in wells containing a finite thickness skin" by C.R. Faust and J.W. Mercer. Water Resources Research, v. 21, no. 9, pp 1459-1461.

Molz, F.J., O. Guven, J.G. Melville, S.J. Nohrstedt, and J.K. Overholtzer. 1988. Forced gradient tracer tests and inferred hydraulic conductivity distributions at the Mobile site. Ground Water. v. 26, no. 5, pp. 570-579.

Moye, D.G. 1967. Diamond drilling for foundation exploration. Civil Engineering Transactions, pp. 95-100.

Muskat, M. 1937. The Flow of Homogeneous Fluids Through Porous Media. McGraw-Hill, New York.

Papadopulos, S.S., J.D. Bredehoeft, and H.H. Cooper. 1973. On the analysis of slug test data. Water Resources Research, v. 9, no. 4, pp. 1087-1089.

Ramey, H.J., Jr. and R.G. Agarwal. 1972. Annulus unloading rates as influenced by wellbore storage and skin effects. Society of Petroleum Engineers Journal, pp. 453-463.

Ramey, H.J., Jr., R.G. Agarwal, and I. Martin. 1975. Analysis of 'slug test' or DST flow period data. Journal of Canadian Petroleum Technology, v. 14, no. 3, pp. 37-47.

Randolph, M.F. and J.R. Booker. 1982. Analysis of seepage into a cylindrical permeameter. Proceedings of the 4th International Conference on Numerical Methods in Geomechanics. Edmonton, v. 1, pp. 349-357.

Raymond, G.P. and M.M. Azzouz. 1969. Permeability determination for predicting rates of consolidation. Institute of Civil Engineers, London, p. 285.

Sageev, A. 1986. Slug test analysis. Water Resources Research, v. 22, no. 8, pp. 1323-1333.

Sheperd, R.G. 1989. Correlations of permeability and grain size. Ground Water, v. 27, no. 5, pp. 633-638.

Smiles, D.E. and E.G. Young. 1965. Hydraulic Conductivity determinations by several field methods in a sand tank. Soil Science, v. 99, no. 2, pp. 83-87.

Tavenas, F.A., M. Tremblay, G. Larouche, and S. Leroueil. 1986a. In situ measurement of permeability in soft clays. Proceedings, ASCE Specialty Conference In Situ '86, Blacksburg, VA. pp. 1034-1048.

Tavenas, F.A., M. Diene, and S. Leroueil. 1986b. Analysis of in situ constant head permeability test. Proceedings, 39th Canadian Geotechnical Conference, Ottawa. pp. 71-77.

Taylor, K., S. Wheatcraft, J. Hess, J. Hayworth, and F. Molz. 1990. Evaluation of methods for determining the vertical distribution of hydraulic conductivity. Ground Water, v. 28, no. 1, pp. 88-98.

Theis, C.V. 1935. The relation between the lowering of the piezometric surface and the rate and duration of discharge of a well using ground-water storage, EOS Trans. AGU, v. 16, pp. 519-524.

van Everdingen, A.F. 1953. The skin effect and its influence in the productive capacity of a well. Transactions, AIME. v. 198, pp. 171-176.

Widdowson, M.A., F.J. Molz, and J.G. Melville. 1990. An analysis technique for multilevel and partially penetrating slug test data. Ground Water, v. 28, no. 6, pp. 937-945.

Wilkinson, W.B. 1968. Constant head in situ permeability tests in clay strata. Geotechnique, v. 18, no. 2, pp. 172-194.

Youngs, E.G. 1968. Shape factors for Kirkham's piezometer method for determining the hydraulic conductivity of soil in situ for soils overlying an impermeable floor or infinitely permeable stratum. Soil Science, v. 106, no. 3, pp. 235-237.

☆U.S. GOVERNMENT PRINTING OFFICE: 1994 - 550-001/80337